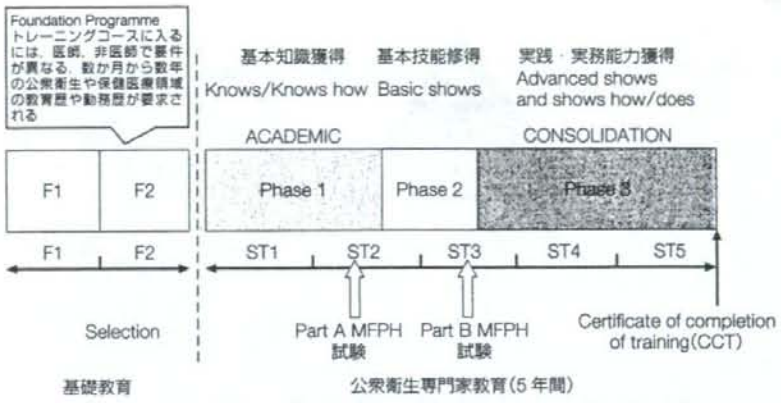

図1　英国における公衆衛生専門職資格修得までの道程

出典：Faculty of Public Health : Public Health Training Curriculum 2007, FPH of RCP, 2007 の中の p 8 の図を参考に高鳥毛が作成.

た．これらの事態に対応するために保健省の Chief Medical Officer であった Sir Donald Acheson を委員長とする委員会が設けられ，英国の公衆衛生体制の現状と，公衆衛生専門職の教育と訓練の現状について検討作業が進められた．最終的に「Public Health in England—The report of the Committee of Inquiry into the future development of the Public Health Function」として 1988 年に報告書としてまとめられた．公衆衛生の仕事をする医師については「public health doctor」と呼ばれるべきであると提言された．これを受け早速，公衆衛生の専門医に関わる王立内科医学会地域医療部(Faculty of Community medicine)の名称は「王立内科医学会公衆衛生医学部(Faculty of Public Health Medicine)」に戻された．"公衆衛生"の言葉が復活し，公衆衛生活動は「人々の健康の保護と増進のために社会が組織的に行う活動である．つまり，国民の健康の脅威となるものを予防し，見つけ出し，取り除き，阻止し，そして，対処する，組織的な努力を行う」ことであると再確認された．これらの仕事を遂行するためには，他の関連分野と密接に連携して活動していかなければならないし，人々の保健ニーズ，予防を含む疾患対策，公衆衛生と医療施策の実績に関する最高の情報を常に保持できるシステムを開発，維持し，実施していくことが必要とされ，公衆衛生人の教育，訓練制度の立て直しについても提言がなされた．

MOH から公衆衛生専門職(家)を中心とした体制への転換

プライマリケア制度改革が進められる中で，それらの組織を指揮する公衆衛生専門職の確保が重要であると認識されてきた．公衆衛生の範囲は通常の NHS の業務を超えるものであり，国や自治体の行政組織，学術領域，軍事関係，さらに地域社会で活動する組織や慈善団体にも関連するものであり，公衆衛生専門職が必要な領域は，保健医療領域を超える多セクターのものであり，技術や専門知識も医学を超える学際的なものであると認識されるようになってきた．1999 年に出された白書「Our Healthier Nation」において，英国の公衆衛生体制の立て直しのためには医師以外の人材も公衆衛生専門職として教育を行い，登用していく必要があるとの方向性が示された．これを受け，2002 年の Primary Care Trust(以下，PCT)における公衆衛生部門の責任者(Director of Public Health)は，医師でなければならないとする要

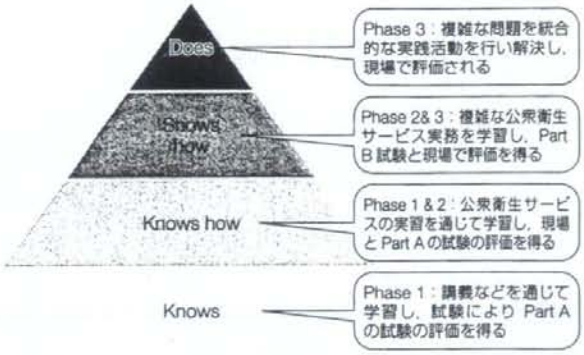

図2　The Miller Triangle(FPH の教育プログラムの中のフェース段階ごとの獲得目標についての模式図)

出典：Miller GE：The assessment of clinical skills/competence/performance. Acad Med **65**(suppl)：S63-67, 1990 を改変

件をなくし，公衆衛生の専門教育を受け，十分に訓練された専門職を充てることとした．公衆衛生の責任者のポストが医師以外の人に拡大されたことに対応して，2003 年に英国王立内科医学会公衆衛生医学部(Faculty of Public Health medicine)の名称から "Medicine" が取り除かれ，「公衆衛生部(Faculty of Public Health：FPH)」と改称された．

公衆衛生専門職(家)とは(図 1，2)

専門職(家)の資格を得るためには，医師の場合，医学部卒業後，前期・後期インターン修了，ジュニア研修医として 3〜6 か月ほど地方のプライマリケアトラストで過ごし，その後，公衆衛生大学院でフルタイムかパートタイムで Master of Science(MSc)や Master in Public Health(MPH)課程を履修する．この期間中の研修医の給与と学費は NHS から全額が支払われる．学科修了時には，英国王立医師会(Royal Collage of Physician)の公衆衛生部門(FPH)の定めた第一部試験(Part A MFPH)がある．第一部試験合格者はシニア研修医となる．3 年間のシニア研修は，ジュニア研修時代とは別の地方の公衆衛生現場に勤務する．シニア研修医の時期に FPH の第二部試験(Part B MFPH)を受ける．第二部試験に合格すると最後に医学高等教育連合委員会から専門医としての資格(Member of Faculty of Public Health：MFPH)が授与される．CCDC(Consultant in Communicable Disease Control)と言われる感染症対策に責任のある専門職は医師に限られている．医師にとっても公衆衛生の専門職となるには長年の教育プログラムを修了しなければならない状況となった．非医師の者が FPH のプログラムに入る場合は公衆衛生に関連する学位(公衆衛生学修士など)，またはそれと同等の学位・資格を有する人，公衆衛生・保健医療関連の職務の実務経験が豊富であることが要求されている．英国を訪れると PCT や HPA(Health Protection Agency)に在籍している非医師の職員が社会人として教育プログラムに参加していた．このことにより医師以外の人々にも公衆衛生専門職(家)の門戸が広く開放され，公衆衛生の有能な専門職をプライマリケアの前線に配置することが可能となってきている．英国の伝統である現場の専門組織に，地域の保健医療問題の解決を委ねることが可能な状況に戻りつつあるように思われる．英国における専門職(MFPH)の資格要件として重視されていることは，公衆衛生に関わる知識を持っているのは当然のことであり，特に実務能力が要求され，特にマネジメント

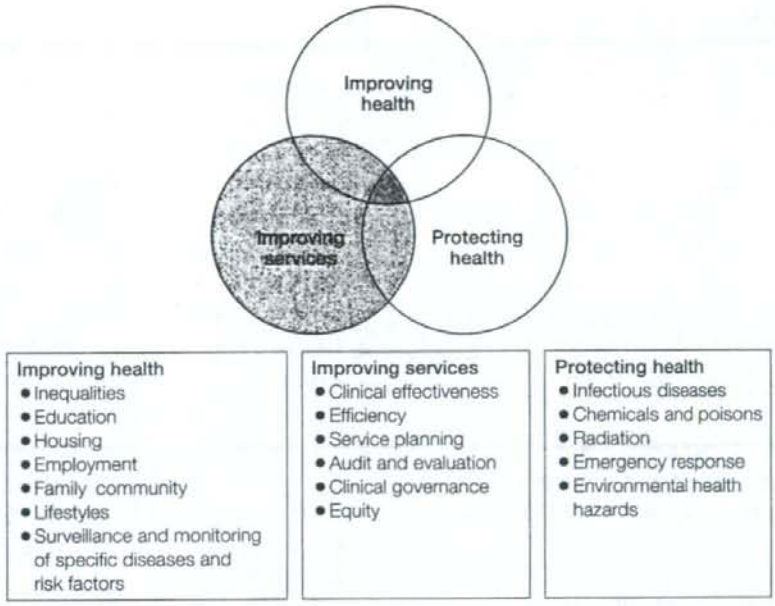

図3　公衆衛生活動の3つの重要な領域

出典：Alison Hill, et al：Public Health and Primary Care Partners in Population Health, Oxford University Press, 2007 の p 19 の Fig. 1.6.

またリーダーシップ能力を持っていることである．

公衆衛生の役割の確認(図3)

NHSの中に保健医官が組み込まれたことにより，プライマリケアと公衆衛生の違いが，保健医官にもわからなくなってしまう状況が生じてきていた．英国においては公衆衛生とプライマリケアは違う役割を担っている存在であり，集合図のように独自に担うものと，重なり合って協働する活動があることが認識されるようになってきた．この状況を感じさせられるのは英国の公衆衛生制度の教科書では「Public Health and Primary Care」と両者を明確に並記したものが目につくようになっていることである．また，公衆衛生には3つの重要な領域があると意識して取り組むべき課題を考えるようになってきていることである．1つ目は健康増進業務(Improving health)，2つ目は保健医療サービスの改善業務(Improving services)，3つ目は健康保護業務(Protecting health)である．

1つ目の健康増進業務(Improving health)の内容はわが国の健康増進業務よりも範囲が広いものであり，健康格差問題の解決を優先課題としている点が特徴となっている．そのような中で，BSEが大きな問題となり，その対応が後手になり，健康被害が拡大してしまっていたことに加え，米国の9.11事件以降のテロ問題への対応も加わってきたことから，これを契機に，公衆衛生組織の抜本的な立て直しに着手していくことになった．2002年にChief Medical Officerによる健康危機管理対策に関する報告書「Getting ahead of the curve」が出され，それに基づき2003年に健康保護機関を，中央組織および地方組織が全国的に整備しはじめ，感染症，化学災害，核・放射線災害に対応する体制が整えられたのである．それがHPAである．英国の公衆衛生組織は，NHSのも

表 Liverpool John Moores University
The Centre for Public Health 修士課程在籍者
(2008年2月)(医学系部門に併設していない大学の例)

・2学年合わせて外国人10人，国内16人在籍
・入学者のプロフィール
　−48%　PCTなどNHSから派遣
　−19%　Local Authoritiesから派遣
　−8%　大学関係
　−11%　Sure Start*
　−14%　Self Private Organization
・3コース
・パートタイムとフルタイムのコースがある．

*The Green Paper「Meeting the Childcare Challenge in 1998」に基づき政府が進める子どものケア対策の推進組織
(Programme Leader Mary Lyons教授のプレゼンテーション資料に基づき高鳥毛が作成したもの)

とにあるPCTが対人保健医療サービスを担い，HPAが感染症対策などの公衆衛生活動を担う，公衆衛生活動の組織が目に見える状況となってきている．

公衆衛生大学院教育の現状

The Royal Commission on Medical Education (通称 Todd Report)において，1965〜68年の3年間，医師全体の卒前・卒後教育について幅広い検討がなされた．その結果，卒後教育の経費について大学は，学術的な学位を目標とする種類の卒後教育については財政負担を担うが，職業教育的な色彩の強い卒後の医師養成課程については，医師の最大の雇用者であるNHSが負担すべきであるとの方向性が出された．大学が貢献する部分については，NHSから大学側にそれに相当する費用の償還をすべきとも勧告がなされた．FPHはこのような医師教育制度改革の中で，公衆衛生医師の職業教育を進めるために，London，Edinburgh，Glasgowの3つのRoyal Colleges of Physicians(RCPs)が合同して1972年に設立したものである．

以上のことが本当なのかどうか確かめるために，平成20年2〜3月に英国の3つの大学を訪問して公衆衛生人職業教育の現状を視察してきた．リーズ大学(国際保健，熱帯医学で有名)，リバプール・ジョンムーア大学(非医学系の私立大学)(表)，グラスゴー大学(歴史のある大学)の3大学を訪問し，プログラム・リーダーの教授や教務主任，学生に会い，英国の公衆衛生人教育の現状をこの目と耳で確かめることができた．英国においては，NHSの機構改革でできたPCT，自治体(Local Authority)，国民の健康保護のための新たなHPAの登場に伴い公衆衛生領域の専門職員の需要が高まり，それに対応して公衆衛生関係の職業教育の制度の確立が不可避な重要課題となってきた大きな背景を理解しておくことが必要である．その職業教育の中心として重要な役割を担ってきたFPHに今まで以上に大きな役割が担わされるようになっていた．FPHは公衆衛生専門職の教育プログラムおよび試験，資格審査を担っている．大学における公衆衛生修士課程の教育プログラムはこのFPHの教育と試験が，認定制度と連動して実施されていた．FPHの資格は，保健医療，公衆衛生領域で仕事をする場合や，SHA (Strategic Health Authority)，またはPCTの中で専門職として地位を得る要件として，健康危機管理組織のHPAの中の専門職としての地位を得るための必要要件と連動して運用されていた．修士課程の学生は，すでに地方自治体の公衆衛生部門やNHSの保健医療分野のスタッフである者の中から，派遣されて勉強している状況にあった．大学のMPHコースにおける実務教育の水準を高めたり，研究委託を行うために教員の人件費を大学外の行政や専門組織が拠出して，寄付講座的に人を雇用することも行われていた．

わが国の公衆衛生人現任教育の課題

公衆衛生学は必然的に専門分化してきている．専門家は研究領域の中だけのことに関心が奪われがちとなる．公衆衛生学の神髄は，それを総合し，社会化すること，国民のものにすることにある．過去30年間，英国社会はこの命題に立ち向かってきたようである．英国における公衆衛生専門職の認定組織はFPHである．「Faculty」とは本来は大学の中の学部の名称であるが，母胎がRoyal Collegesなので Facultyという名称となっ

ているようである．既存の行政や大学や学会などとは独立した組織である．大学などの教育組織のようにシラバス，教育プログラムの作成，公衆衛生実務に関わるガイドラインの策定，研究会や研修会を開催している．それに加えて，資格試験と資格認定と資格の授与，研究や出版物の発行を行っている．Academic な学問の教育を担っている大学の Faculty とは別に，Profession の教育という重要な社会的役割を担っている実社会の必要な人材育成のための教育機関とも言える．王立という形容詞をつけているが，それは王家一族の誰かを名目上のスポンサーにいただくというだけのことであって，実質的には王家とも政府とも関係のない民間の職能・学術団体である．専門職を位置づける環境を有する英国の象徴的な組織のように思われる．わが国にはこのような問題を取り上げ検討する機構が存在していない．

わが国は近年ようやく自立した地方自治体の育成をめざして，地方分権が進められてきている．この流れは止めようのないものとなっている．保健行政，公衆衛生行政の主体も自治体が担う流れとなり，保健所も指定都市，中核市へと移管されてきている．とかく公衆衛生関係者はこの流れを否定的に受け止めがちであるが，自治体の中で公衆衛生専門職が公衆衛生対策を担っていく時代は不可避な現実となっている．それが故に，わが国もこれまで以上に自治体における公衆衛生専門職員の現任教育が重要となってきている．英国のように，何らかの教育体制を国や学会だけではなく，社会全体が力を傾注して作っていかなければならない状況になっているのではないだろうか．

文　献

1）張知夫：卒後教育をどうするか．関悌四郎(編)：集団医学の発足．pp 177-216．現代ジャーナリズム出版会，1970
2）Department of Health : Public Health in England. Report of the Committee of Inquiry into the Future Development of the Public Health Function. London, 1988
3）John Ashton, Howard Seymour : The New Public Health. pp 15-40, The Setting for a New Public Health, 1990
4）今村恭子，水嶋春朔：イギリスの公衆衛生専門教育．公衆衛生 62(3)：195-200，1998
5）多田羅浩三：公衆衛生の思想　歴史からの教訓．pp 251-255．医学書院，1999
6）Department of Health : Getting ahead of the curve ; A strategy for combatting infectious diseases (including other aspects of health protection). London, 2002
7）林謙治：リーダーシップの養成―英米との対比から．公衆衛生 68(1)：31-34，2004
8）高鳥毛敏雄：ロンドンの公衆衛生体制と結核対策戦略．公衆衛生 69(3)：203-208，2005
9）Alison Hill, Sian Griffiths, Stephen Gillam : Public Health and Primary Care Partners in Population Health. Oxford University Press, 2007
10）Faculty of Public Health of the Royal Colleges of physicians of the United Kingdom : Public Health Training Curriculum 2007. pp 1-70, FPH of RCP, 2007
11）Bradford and Airedale NHS Teaching Primary Care Trust : The Annual Report of the Joint Director of Public Health, Bradford and Airedale 2007/2008, Bradford District Council, 2008

doi:10.1038/nature07240

LETTERS

ATP drives lamina propria T_H17 cell differentiation

Koji Atarashi[1]*, Junichi Nishimura[1]*, Tatsuichiro Shima[2], Yoshinori Umesaki[2], Masahiro Yamamoto[1,3], Masaharu Onoue[2], Hideo Yagita[4], Naoto Ishii[5], Richard Evans[6], Kenya Honda[1,3] & Kiyoshi Takeda[1,3]

Interleukin (IL)-17-producing $CD4^+$ T lymphocytes (T_H17 cells) constitute a subset of T-helper cells involved in host defence and several immune disorders[1,2]. An intriguing feature of T_H17 cells is their selective and constitutive presence in the intestinal lamina propria[3]. Here we show that adenosine 5′-triphosphate (ATP) that can be derived from commensal bacteria activates a unique subset of lamina propria cells, $CD70^{high}CD11c^{low}$ cells, leading to the differentiation of T_H17 cells. Germ-free mice exhibit much lower concentrations of luminal ATP, accompanied by fewer lamina propria T_H17 cells, compared to specific-pathogen-free mice. Systemic or rectal administration of ATP into these germ-free mice results in a marked increase in the number of lamina propria T_H17 cells. A $CD70^{high}CD11c^{low}$ subset of the lamina propria cells expresses T_H17-prone molecules, such as IL-6, IL-23p19 and transforming-growth-factor-β-activating integrin-αV and -β8, in response to ATP stimulation, and preferentially induces T_H17 differentiation of co-cultured naive $CD4^+$ T cells. The critical role of ATP is further underscored by the observation that administration of ATP exacerbates a T-cell-mediated colitis model with enhanced T_H17 differentiation. These observations highlight the importance of commensal bacteria and ATP for T_H17 differentiation in health and disease, and offer an explanation of why T_H17 cells specifically present in the intestinal lamina propria.

The intestinal mucosa has a unique and complicated immune system composed of a variety of cell populations. Among these, T_H17 cells, a subset of $CD4^+$ T cells characterized by their STAT3-dependent expression of RORγt (encoded by *Rorc*) and production of IL-17, IL-22 and IL-21, control a variety of bacterial and fungal infections at mucosal surfaces[1–7]. Importantly, aberrant T_H17 responses have been implicated in the pathogenesis of inflammatory bowel diseases[8]. The development of T_H17 cells has been shown to be controlled by the local cytokine milieu, including IL-6, transforming growth factor-β (TGF-β) and IL-23 (refs 1, 2, 7, 9–12). However, the mechanism of T_H17 development in the intestine is as yet not fully understood.

IL-17-expressing cells constitute a considerable proportion of $CD4^+$ cells in the intestinal lamina propria, even in healthy mice kept under specific-pathogen-free (SPF) conditions (Supplementary Fig. 1a and ref. 3). The colonic lamina propria $CD4^+$ cells also express messenger RNAs for IL-17, IL-17F and RORγt, representing the hallmarks of T_H17 cells (Supplementary Fig. 1b). The number of these 'naturally occurring' T_H17 cells in the colonic lamina propria increases with age (Supplementary Fig. 1c). Although interferon (IFN)-γ-positive $CD4^+$ cells are similarly observed in the lamina propria and spleen, IL-17-producing cells are rarely observed in the spleen, mesenteric lymph node (MLN) or Peyer's patches (Supplementary Fig. 1a and ref. 3). Furthermore, the lamina propria IL-17-producing $CD4^+$ cells were normally observed in Peyer's-patch- and colonic-patch-null mice[13] (Supplementary Fig. 2). These observations suggest that a specific environment in the lamina propria supports the generation of T_H17 cells *in situ*.

To investigate whether intestinal commensal bacteria are responsible for the generation of lamina propria T_H17 cells, we evaluated the numbers of T_H17 cells in germ-free mice. Although the numbers of colonic lamina propria $CD4^+$ cells were not significantly changed (Supplementary Fig. 3a), the numbers of IL-17-positive $CD4^+$ cells were greatly reduced in the large intestines of germ-free mice compared to those in SPF mice (Fig. 1a, b and Supplementary Fig. 3b). Consistent with previous reports[14], the germ-free mice also exhibited severe reductions in their faecal IgA levels (Supplementary Fig. 3c), demonstrating that commensal bacteria contribute to the provision of a particular environment for lamina propria T_H17 cells as well as IgA-producing cells. To examine the role of commensal bacteria further, we treated SPF mice with a combination of vancomycin and metronidazole by oral administration, and analysed lamina propria T_H17 cells. The vancomycin- and metronidazole-treated mice showed marked reductions in both their faecal IgA levels and their numbers of IL-17-producing $CD4^+$ cells (Supplementary Fig. 4a–c).

To assess the molecular basis for the commensal-bacteria-driven T_H17 differentiation, we examined the contribution of Toll-like receptor (TLR) signalling using $Myd88^{-/-}Trif^{-/-}$ mice, which lack all TLR signalling. There was no detectable difference in the numbers of lamina propria IL-17-producing $CD4^+$ cells between control and mutant animals (Fig. 1c, d and Supplementary Fig. 3d), indicating that the development of lamina propria T_H17 cells is independent of TLR signalling. It is worth noting that $Myd88^{-/-}Trif^{-/-}$ mice showed impaired secretion of IgA in their faecal pellets (Supplementary Fig. 3e), indicating that the development of intestinal T_H17 cells and IgA-producing cells are both dependent on microflora, but are regulated by different mechanisms.

ATP has recently been shown to modulate immune cell functions by means of activation of the ATP sensors, P2X and P2Y receptors[15–18]. In addition, bacteria have been shown to generate and secrete large amounts of ATP[19]. Indeed, ATP concentrations in faecal samples without bacterial lysis were much higher in SPF mice than in germ-free mice (Fig. 1e). Consistent with this result, ATP concentrations were reduced in faecal samples from SPF mice treated with vancomycin and metronidazole (Supplementary Fig. 4d). Furthermore, high ATP concentration was detected in the supernatant of *in vitro* cultured intestinal commensal bacteria derived from faeces of SPF mice (Supplementary Fig. 5). Therefore, although there might be other cellular sources of ATP such as dead epithelial cells, commensal bacteria may be a major source of intestinal luminal ATP. Interestingly, the faecal ATP concentrations were not reduced in

[1]Laboratory of Immune Regulation, Graduate School of Medicine, Osaka University, 2-2 Yamadaoka, Suita, Osaka 565-0871, Japan. [2]Yakult Central Institute for Microbiological Research, Yaho 1796, Kunitachi, Tokyo 186-8650, Japan. [3]WPI Immunology Frontier Research Center, Osaka University, Osaka 565-0871, Japan. [4]Department of Immunology, Juntendo University School of Medicine, 2-1-1 Hongo, Bunkyo-ku, Tokyo 113-8421, Japan. [5]Department of Microbiology and Immunology, Tohoku University Graduate School of Medicine, 2-1 Seiryo-machi, Aoba-ku, Sendai 980-8575, Japan. [6]Department of Cell Physiology and Pharmacology, Henry Wellcome Building 2/59b, University of Leicester, Leicester LE1 9HN, UK.
*These authors contributed equally to this work.

Myd88$^{-/-}$ *Trif*$^{-/-}$ mice (Fig. 1f). These results prompted us to examine the contribution of ATP to the generation of intestinal T_H17 cells. To this end, we treated germ-free mice with a non-hydrolysable ATP analogue, ATPγS (ref. 15), by intraperitoneal or rectal administration, and analysed the numbers of lamina propria IL-17-producing cells. The numbers of IL-17-producing CD4$^+$ cells were markedly increased in the ATPγS-treated germ-free mice (Fig. 1g–i). In contrast, ATP injection affected neither the numbers of IFN-γ-producing CD4$^+$ cells (Fig. 1g, h) nor faecal IgA levels (Supplementary Fig. 3f). To assess further the possible involvement of ATP in T_H17 differentiation, we treated SPF mice with an ATP-hydrolysing enzyme, apyrase, or with an antagonist of P2X receptors, 2′,3′-*O*-(2,4,6-trinitrophenyl)-ATP (TNP-ATP)[15]. In the apyrase- or TNP-ATP-treated mice, the numbers of IL-17-producing lamina propria CD4$^+$ cells were significantly reduced (Fig. 1j, k), suggesting the key role of ATP in the generation of intestinal T_H17 cells.

Accumulating evidence suggests that lamina propria CD11c$^+$ antigen-presenting cells directly sample the luminal contents and activate T cells[20,21]. Indeed, the induction of mRNAs for IL-6 (encoded by *Il6*), IL-23p19 (*Il23a*) and integrin-αV (*Itgav*) and -β8 (Itgb8) was observed in lamina propria CD11c$^+$ cells, but not in CD11c$^-$ cells or epithelial cells, harvested from ATPγS-treated germ-free mice (Supplementary Fig. 6). Integrin-αV and -β8 are known to be involved in the activation of latent complexes of TGF-β[22]. Therefore, we assumed that ATP promotes T_H17 differentiation by means of stimulation of lamina propria CD11c$^+$ cells. Accordingly, we next co-cultured lamina propria CD11c$^+$ cells with splenic naive CD4$^+$CD62L$^+$ T cells in the presence of a culture supernatant of intestinal commensal bacteria, which contained a high amount of ATP (Supplementary Fig. 5). Addition of this supernatant markedly enhanced differentiation of IL-17-expressing cells, but not of IFN-γ-expressing cells (Fig. 2a). This T_H17 differentiation was severely inhibited by the presence of apyrase. In contrast, a culture supernatant from *Salmonella typhimurium* showed a lower concentration of ATP and weaker ability to induce T_H17 differentiation (Fig. 2a and Supplementary Fig. 5). Notably, the culture supernatant from *S. typhimurium* potently induced T_H1 differentiation, but this was not inhibited by apyrase (Fig. 2a).

To assess whether ATP was sufficient to induce T_H17 differentiation, we co-cultured lamina propria or splenic CD11c$^+$ cells with splenic naive CD4$^+$ cells in the presence of ATPγS. The expression levels of *Il17a*, *Il17F*, *Il21* and *Il22*, but not *Ifng*, were markedly increased in CD4$^+$ cells cultured with lamina propria CD11c$^+$ cells in the presence of ATPγS (Fig. 2b and Supplementary Fig. 7a). The T_H17 differentiation was also enhanced by another non-hydrolysable form of ATP, α,β-methylene-ATP (αβ-ATP), and weakly enhanced by 2,3-*O*-(4-benzoylbenzoyl)-ATP (Bz-ATP)[15] (Supplementary Fig. 7b). *Myd88*$^{-/-}$ *Trif*$^{-/-}$ CD11c$^+$ cells and control cells exerted a similar effect on CD4$^+$ cells, ruling out the possibility of endotoxin contamination (Supplementary Fig. 7c). The effect by ATPγS or αβ-ATP on T_H17 differentiation was inhibited by pharmacological blockade of P2X and P2Y receptors using suramin, or a combination of TNP-ATP and brilliant blue G[15] (Supplementary Fig. 8). Importantly, these inhibitors had no effect

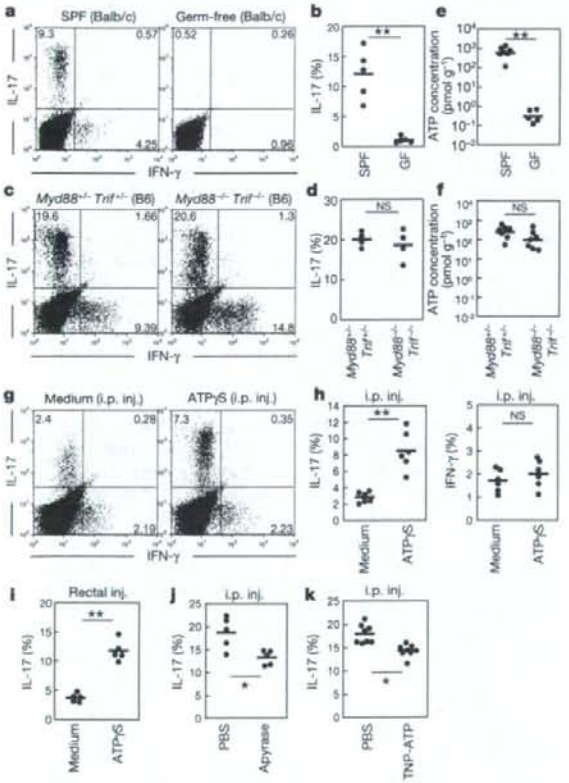

Figure 1 | Administration of ATP leads to a marked increase in lamina propria T_H17 cells in otherwise T_H17-lacking germ-free mice. **a**–**d**, Representative FACS dot plots gated on colonic lamina propria CD4$^+$ cells in the indicated mice are shown in **a** and **c**, and the percentages of IL-17-producing CD4$^+$ cells of individual mice are shown in **b** and **d**. GF, germ free. **e**, **f**, Faecal ATP levels (pmol per g faeces) in the indicated individual mice. **g**–**k**, Germ-free mice (ICR) were daily injected intraperitoneally (i.p.) or rectally with medium or ATPγS (**g**–**i**). SPF mice were i.p. injected with PBS or apyrase, or with TNP-ATP (**j**, **k**). All mice were processed for FACS as in **a**–**d**. All experiments were performed more than twice with similar results. Horizontal bars indicate the means. $^{**}P < 0.01$, $^{*}P < 0.05$; NS, not significant.

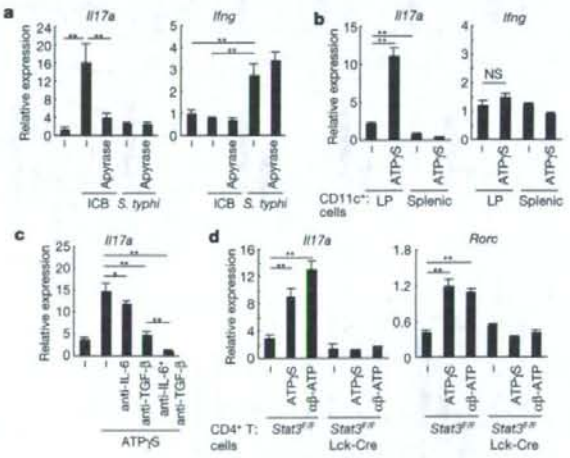

Figure 2 | ATP induces differentiation of naive CD4$^+$ T cells into T_H17 cells. **a**, Splenic naive CD4$^+$ T cells were co-cultured with colonic lamina propria CD11c$^+$ with 20% conditioned medium from cultures of intestinal commensal bacteria (ICB) or *S. typhimurium* (*S. typhi*) in the presence or absence of apyrase. After 4 days, T cells were collected, restimulated and assayed for expression of *Il17* and *Ifng* by rRT–PCR. **b**, **c**, rRT–PCR analyses for the indicated genes of splenic naive CD4$^+$ T cells cultured with colonic lamina propria (LP) or splenic CD11c$^+$ cells in the presence of ATPγS (**b**) with or without anti-IL-6, anti-TGF-β or their combination (**c**). **d**, rRT–PCR analyses for the indicated genes of splenic naive CD4$^+$ T cells from *Stat3*$^{F/F}$ Lck-Cre or *Stat3*$^{F/F}$ mice cultured with wild-type colonic LP CD11c$^+$ cells in the presence of ATPγS or αβ-ATP. Error bars, s.d. $^{*}P < 0.05$, $^{**}P < 0.01$. Representative results are shown from one of two to five independent experiments.

on, or slightly enhanced, T_H1 cell differentiation. Although there might be other molecules affected by the ATP analogues and inhibitors we used, our results support the notion that the specific effect of ATP on T_H17 differentiation was mediated by P2X and P2Y receptors. The ATP-mediated enhancement of T_H17 differentiation was inhibited by anti-IL-6 or anti-TGF-β antibodies, and more severely inhibited by the combination of both antibodies (Fig. 2c). Consistent with this result, *Il6*$^{-/-}$ CD11c$^+$ cells failed to induce the differentiation of IL-17-producing cells in response to ATP (Supplementary Fig. 7d). In addition, no effects of ATP on the differentiation of cells expressing *Il17a* and *Rorc* were observed for CD4$^+$ cells from *Stat3*$^{F/F}$ mice crossed onto Lck-Cre mice (*Stat3*$^{F/F}$ Lck-Cre mice), in which the *Cre* transgene is under the control of the *Lck* promoter[23] (Fig. 2d). These results suggest that ATP stimulates lamina propria CD11c$^+$ cells to produce IL-6 and TGF-β, thereby promoting the T_H17 differentiation by activation of STAT3 in CD4$^+$ cells.

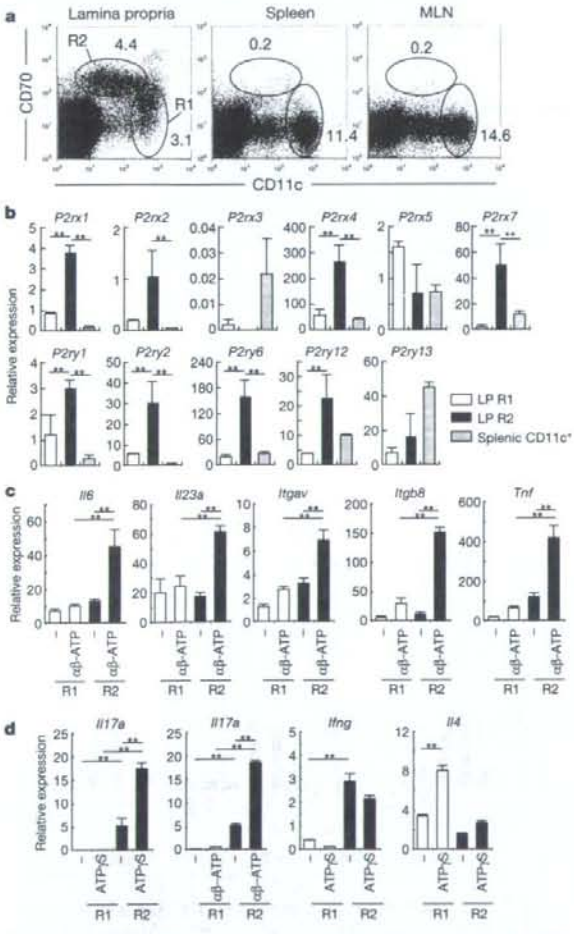

Figure 3 | A unique subset of lamina propria CD11c$^+$ cells express P2X and P2Y receptors. a, Flow cytometry of cells isolated from the colonic lamina propria, spleen or MLN. Numbers indicate the percentages of CD70^{low}CD11c^{high} cells (R1) or CD70^{high}CD11c^{low} cells (R2). **b**, rRT–PCR analyses for P2X and P2Y receptors in R1, R2 or splenic CD11c$^+$ cells. **c**, The sorted R1 and R2 cells were stimulated with αβ-ATP for 3 h and assayed for expression of the indicated genes. **d**, The sorted R1 and R2 cells were co-cultured with splenic naive CD4$^+$ T cells with ATPγS or αβ-ATP for 4 days. The levels of indicated mRNAs in the co-cultured T cells were analysed by rRT–PCR. Data are presented as means + s.d. of triplicate determinations. All experiments were performed more than three times with similar results. $^{**}P < 0.01$.

The heterogeneity of lamina propria CD11c$^+$ cells has been addressed in a number of studies[24]. Therefore, we investigated which subsets of lamina propria CD11c$^+$ cells mediate T_H17 development. Flow cytometry analyses led to the identification of two major CD11c$^+$ populations in the colonic lamina propria: CD70^{low}CD11c^{high} cells (termed R1) and CD70^{high}CD11c^{low} cells (termed R2; Fig. 3a). The R2 population comprised a unique subset present in the lamina propria (Fig. 3a). This subset was positive for myeloid lineage cell markers, such as F4/80 and CD11b, and exhibited immune-activating properties, as was evident from their high expression of CD70 and CD80, but was negative for the immune-suppressive marker CD103 (Supplementary Fig. 9a and refs 25 and 26). R2 cells also expressed CX3CR1; thus, this population seems to be a part of the previously described CX3CR1$^+$CD11b^{high}CD11c^{low} T_H17-inducing subset[26] (Supplementary Fig. 9a–c). R2 cells were observed in the lamina propria of germ-free mice or Peyer's-patch- and colonic-patch-null mice (Supplementary Fig. 11a, b), suggesting that this subset of cells develop by means of microflora- and Peyer's-patch-/colonic-patch-independent mechanisms. Because treatment with a blocking antibody for CD70 or deficiency of CD27, a receptor for CD70 (ref. 27), did not influence the number of lamina propria T_H17 cells (data not shown), CD70 itself is dispensable for T_H17 differentiation.

Next, we sorted R1 or R2 cells (Supplementary Fig. 10) and examined their expression of P2X and P2Y receptors by real-time polymerase chain reaction with reverse transcription (rRT–PCR). R2 cells expressed higher levels of mRNA for P2X1, P2X2, P2X4, P2X7, P2Y1, P2Y2, P2Y6 and P2Y12 receptors than R1 cells or splenic CD11c$^+$ cells (Fig. 3b). Furthermore, R2 cells expressed *Il6*, *Il23a Itgav* and *Itgb8* in response to ATP (Fig. 3c). In addition, on ATP stimulation, R2 cells expressed tumour necrosis factor-α (TNF-α), which has been implicated in T_H17 responses in humans[28]. R2 cells, but not R1 cells, efficiently induced the differentiation of co-cultured naive CD4$^+$CD62L$^+$ T cells into IL-17-expressing cells, and this effect was markedly enhanced by the presence of ATP (Fig. 3d). Although the R2 population also induced T cells to differentiate into IFN-γ-positive cells, this effect was not enhanced by ATPγS (Fig. 3d). In this experimental setting, IL-4-expressing cells were also induced, but this effect was more remarkable in co-cultures with R1 cells, suggesting that R1 and R2 cells carry out distinct missions with each other. R2 cells present in germ-free mice expressed low levels of *Il6* and *Itgb8*, and showed lower ability to induce T_H17 differentiation of co-cultured naive CD4$^+$ T cells (Supplementary Fig. 11c, d); however, by the addition of ATPγS, R2 cells from germ-free mice efficiently enhanced the T_H17 differentiation (Supplementary Fig. 11d). These results all support the hypothesis that commensal-bacteria-derived ATP is responsible for the activation of R2 cells and subsequent development of T_H17 cells.

To extend our understanding of the role of ATP in the differentiation of T_H17 cells, we examined the effects of ATP on intestinal inflammation. We adoptively transferred naive wild-type CD4$^+$ T cells into severe combined immunodeficient (SCID) mice[29], treated these mice with αβ-ATP or medium, and monitored the severity of their colitis. Although both groups developed colitis, treatment with αβ-ATP exacerbated the symptoms of the disease, including diarrhoea and weight loss (Fig. 4a, Supplementary Fig. 12a and data not shown). Extensive oedema was prominent in the colon of αβ-ATP-treated SCID mice (Supplementary Fig. 12b). Histological analyses revealed that inflammatory cell infiltration, epithelial hyperplasia and loss of goblet cells were more evident in the colon of αβ-ATP-treated SCID mice (Fig. 4b). Notably, in contrast to a lack of considerable effect on IFN-γ-positive cells, the number of IL-17-positive CD4$^+$ cells was significantly increased in the αβ-ATP-treated SCID mice (Fig. 4c, d and Supplementary Fig. 12c). Thus, ATP-induced deterioration of colitis was accompanied by an increase in the

number of T_H17 cells in this T-cell-mediated colitis model, indicating the possible involvement of ATP in the generation of 'pathogenic' T_H17 cells.

From our results, we propose the following scenario: commensal-bacteria-derived ATP activates $CD70^{high}CD11c^{low}$ cells in the lamina propria to induce IL-6 and IL-23 production as well as TGF-β activation, thereby leading to local differentiation of T_H17 cells. Our findings further suggest that this mechanism commonly operates during the differentiation of both 'naturally occurring' and 'pathogenic' T_H17 cells, although additional factors certainly contribute differentially to each case[30]. The physiological nature and role of these T_H17 cells will be an interesting issue to be addressed in the context of the maintenance of intestinal mucosal homeostasis[10,12]. The actual involvement of P2 receptors and subsequent intracellular signalling mechanisms responsible for the generation of the local cytokine milieu inducing T_H17 cells are also interesting issues for future studies. Finally, elucidating the entire picture of the development of intestinal regulatory T cells, T_H17 cells and other types of cells by ATP and its metabolites (ADP and adenosine) will provide valuable information towards our understanding of the complex system of intestinal mucosal immunity as well as the establishment of innovative ATP-targeted approaches for treating patients with inflammatory bowel diseases.

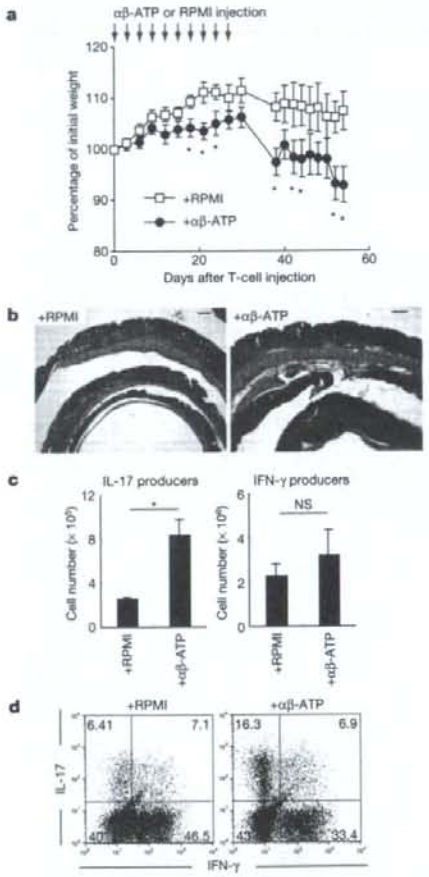

Figure 4 | Treatment with ATP exacerbates experimental colitis induced by adoptive transfer of naive $CD4^+$ T cells. SCID mice were transferred with naive $CD4^+$ T cells on day 0, and were intraperitoneally injected with αβ-ATP (1.5 mg per mouse) or RPMI 1640 medium every 3 days for 1 month. **a**, The mean body weights of SCID mice injected with αβ-ATP or RPMI ($n = 6$ per group) were monitored. Error bars, s.e.m. $^*P < 0.05$ versus RPMI-injected mice. **b**, Haematoxylin- and eosin-stained colon sections of SCID mice treated with αβ-ATP or RPMI. The numbers of IL-17- and IFN-γ-producing colonic lamina propria $CD4^+$ cells ($n = 3$ per group) are shown in **c**, and representative flow cytometry plots of $CD4^+$ T cells are shown in **d**. Error bars, s.d. $^*P < 0.02$. NS, not significant. Two independent experiments were performed with similar results.

METHODS SUMMARY

Mice, cell isolation and faecal ATP measurements. C57BL/6J mice, CB-17 SCID mice and ICR germ-free mice were purchased from CLEA Japan. Balb/c germ-free mice were maintained at the Yakult Central Institute. *Myd88*$^{-/-}$, *Trif*$^{-/-}$ and *Stat3*$^{F/F}$ Lck-Cre mice backcrossed eight or more generations onto C57BL/6J were used. The details of the procedures for isolation of lamina propria lymphocytes and $CD11c^+$ cells are described in Methods. Faeces from individual mice were weighed and suspended in PBS. The levels of ATP in the supernatants were determined with a luciferin-luciferase assay using an ATP assay kit (TOYO Ink.).

Intracellular cytokine staining and *in vitro* T-cell differentiation. The details of the procedures for intracellular cytokine staining and *in vitro* differentiation of $CD4^+$ T cells are described in Methods.

rRT–PCR. The details of the procedures and primers used for rRT–PCR are described in Methods. For all panels, bars represent the ratio of gene to *Gapdh* expression as determined by the relative quantification method (ΔΔCT) (mean + s.d. of triplicate determination).

T-cell-mediated colitis model. Naive $CD4^+CD62L^{high}$ splenic T cells from Balb/c mice were intraperitoneally transferred into SCID mice (3×10^5 cells per mouse). The mice were then injected with αβ-ATP (1.5 mg per mouse) or medium alone every 3 days for 4 weeks. After 6 or 8 weeks, colons were analysed.

Statistical analysis. Differences between control and experimental groups were evaluated using Student's *t*-test.

Full Methods and any associated references are available in the online version of the paper at www.nature.com/nature.

Received 4 June; accepted 7 July 2008.
Published online 20 August 2008.

1. Weaver, C. T., Hatton, R. D., Mangan, P. R. & Harrington, L. E. IL-17 family cytokines and the expanding diversity of effector T cell lineages. *Annu. Rev. Immunol.* **25**, 821–852 (2007).
2. Bettelli, E., Oukka, M. & Kuchroo, V. K. T_H-17 cells in the circle of immunity and autoimmunity. *Nature Immunol.* **8**, 345–350 (2007).
3. Ivanov, I. I. *et al.* The orphan nuclear receptor RORγt directs the differentiation program of proinflammatory IL-17$^+$ T helper cells. *Cell* **126**, 1121–1133 (2006).
4. Liang, S. C. *et al.* Interleukin (IL)-22 and IL-17 are coexpressed by Th17 cells and cooperatively enhance expression of antimicrobial peptides. *J. Exp. Med.* **203**, 2271–2279 (2006).
5. Nurieva, R. *et al.* Essential autocrine regulation by IL-21 in the generation of inflammatory T cells. *Nature* **448**, 480–483 (2007).
6. Korn, T. *et al.* IL-21 initiates an alternative pathway to induce proinflammatory T_H17 cells. *Nature* **448**, 484–487 (2007).
7. Zhou, L. *et al.* IL-6 programs T_H-17 cell differentiation by promoting sequential engagement of the IL-21 and IL-23 pathways. *Nature Immunol.* **8**, 967–974 (2007).
8. Cho, J. H. & Weaver, C. T. The genetics of inflammatory bowel disease. *Gastroenterology* **133**, 1327–1339 (2007).
9. Veldhoen, M., Hocking, R. J., Atkins, C. J., Locksley, R. M. & Stockinger, B. TGFβ in the context of an inflammatory cytokine milieu supports *de novo* differentiation of IL-17-producing T cells. *Immunity* **24**, 179–189 (2006).
10. Mangan, P. R. *et al.* Transforming growth factor-β induces development of the T_H17 lineage. *Nature* **441**, 231–234 (2006).
11. Bettelli, E. *et al.* Reciprocal developmental pathways for the generation of pathogenic effector T_H17 and regulatory T cells. *Nature* **441**, 235–238 (2006).
12. Cua, D. J. & Kastelein, R. A. TGF-β, a 'double agent' in the immune pathology war. *Nature Immunol.* **7**, 557–559 (2006).
13. Chang, S. Y. *et al.* Colonic patches direct the cross-talk between systemic compartments and large intestine independently of innate immunity. *J. Immunol.* **180**, 1609–1618 (2008).
14. Fagarasan, S. & Honjo, T. Intestinal IgA synthesis: regulation of front-line body defences. *Nature Rev. Immunol.* **3**, 63–72 (2003).
15. North, R. A. Molecular physiology of P2X receptors. *Physiol. Rev.* **82**, 1013–1067 (2002).
16. Schnurr, M. *et al.* Extracellular nucleotide signaling by P2 receptors inhibits IL-12 and enhances IL-23 expression in human dendritic cells: a novel role for the cAMP pathway. *Blood* **105**, 1582–1589 (2005).
17. Khakh, B. S. & North, R. A. P2X receptors as cell-surface ATP sensors in health and disease. *Nature* **442**, 527–532 (2006).
18. Idzko, M. *et al.* Extracellular ATP triggers and maintains asthmatic airway inflammation by activating dendritic cells. *Nature Med.* **13**, 913–919 (2007).

19. Ivanova, E. P., Alexeeva, Y. V., Pham, D. K., Wright, J. P. & Nicolau, D. V. ATP level variations in heterotrophic bacteria during attachment on hydrophilic and hydrophobic surfaces. *Int. Microbiol.* **9**, 37–46 (2006).
20. Rescigno, M. *et al.* Dendritic cells express tight junction proteins and penetrate gut epithelial monolayers to sample bacteria. *Nature Immunol.* **2**, 361–367 (2001).
21. Niess, J. H. *et al.* CX3CR1-mediated dendritic cell access to the intestinal lumen and bacterial clearance. *Science* **307**, 254–258 (2005).
22. Travis, M. A. *et al.* Loss of integrin alpha(v)beta8 on dendritic cells causes autoimmunity and colitis in mice. *Nature* **449**, 361–365 (2007).
23. Takeda, K. *et al.* Stat3 activation is responsible for IL-6-dependent T cell proliferation through preventing apoptosis: generation and characterization of T cell-specific Stat3-deficient mice. *J. Immunol.* **161**, 4652–4660 (1998).
24. Iwasaki, A. Mucosal dendritic cells. *Annu. Rev. Immunol.* **25**, 381–418 (2007).
25. Coombes, J. L. *et al.* A functionally specialized population of mucosal CD103$^+$ DCs induces Foxp3$^+$ regulatory T cells via a TGF-β and retinoic acid-dependent mechanism. *J. Exp. Med.* **204**, 1757–1764 (2007).
26. Denning, T. L., Wang, Y. C., Patel, S. R., Williams, I. R. & Pulendran, B. Lamina propria macrophages and dendritic cells differentially induce regulatory and interleukin 17-producing T cell responses. *Nature Immunol.* **8**, 1086–1094 (2007).
27. Hendriks, J. *et al.* CD27 is required for generation and long-term maintenance of T cell immunity. *Nature Immunol.* **1**, 433–440 (2000).
28. Zaba, L. C. *et al.* Amelioration of epidermal hyperplasia by TNF inhibition is associated with reduced Th17 responses. *J. Exp. Med.* **204**, 3183–3194 (2007).
29. Leach, M. W., Bean, A. G., Mauze, S., Coffman, R. L. & Powrie, F. Inflammatory bowel disease in C.B-17 scid mice reconstituted with the CD45RB^{high} subset of CD4$^+$ T cells. *Am. J. Pathol.* **148**, 1503–1515 (1996).
30. Mazmanian, S. K., Round, J. L. & Kasper, D. L. A microbial symbiosis factor prevents intestinal inflammatory disease. *Nature* **453**, 620–625 (2008).

Supplementary Information is linked to the online version of the paper at www.nature.com/nature.

Acknowledgements We thank A. Iwasaki and N. Tsuji for discussion, M. H. Jang, H. Ohno, H. Yamane, M. Yoshida and H. Shiomi for technical advice and reagents, and J. Borst for CD27-deficient mice. This work was supported by Grants-in-Aid from the Ministry of Education, Culture, Sports, Science and Technology, the Ministry of Health, Labour and Welfare, the Osaka Foundation for the Promotion of Clinical Immunology, the Ichiro Kanehara Foundation, Sumitomo Foundation, Senri Life Science Foundation and the Naito Foundation.

Author Contributions K.H. conceived the research, planned experiments and analyses and wrote the paper; K.A. and J.N. largely conducted experiments; T.S. performed some of the experiments; Y.U., M.Y., M.O., H.Y., N.I. and R.E. provided key materials; and K.T. oversaw the whole project.

Author Information Reprints and permissions information is available at www.nature.com/reprints. Correspondence and requests for materials should be addressed to K.H. (honda@ongene.med.osaka-u.ac.jp) or K.T. (ktakeda@ongene.med.osaka-u.ac.jp).

METHODS

Reagents. ATPγS (A1388), αβ-ATP (M6517) and Bz-ATP (B6396) were purchased from Sigma-Aldrich, and dissolved in phenol-red-free RPMI1640 medium. Apyrase from potato (ATPase activity: 40–200 units (U) per mg protein, A7646), suramine (S2671), TNP-ATP (T4193) and BBG (B0770) were purchased from Sigma-Aldrich, and dissolved in PBS. For *in vivo* experiments, 80 U apyrase or 250 μg of TNP-ATP was dissolved in 300 μl PBS and immediately injected intraperitoneally into SPF mice every 3 days for 15 days; or 1.25 mg of ATPγS was dissolved in phenol-red-free RPMI1640 medium and injected daily intraperitoneally or intrarectally with syringes or 1,000-μl pipette tips, respectively, into germ-free mice for 6 days. For *in vitro* experiments, ATPγS, αβ-ATP and Bz-ATP were used at 5–10 μM; suramin at 30 μM; TNP-ATP at 10 μM; BBG at 100 nM; and apyrase at 15 U ml^{-1}. The anti-IL-6 and anti-TGF-β antibodies were purchased from R&D Systems and used at 10 μg ml^{-1} or 25 μg ml^{-1}, respectively.

Mice. CB-17 SCID mice and ICR germ-free mice were purchased from CLEA Japan. Balb/c germ-free mice were maintained at the Yakult Central Institute. *Myd88*$^{-/-}$, *Trif*$^{-/-}$ and *Stat3*$^{F/F}$ Lck-Cre mice were generated as described previously[23,31], and backcrossed eight or more generations onto C57BL/6J. CD27-deficient mice were used with permission from J. Borst[27]. Unless otherwise indicated, wild-type C57BL/6J mice purchased from CLEA Japan maintained under SPF conditions were used. All experiments were performed in accordance with the Guidelines for Animal Experiments of Osaka University.

Faecal ATP measurements. Faeces from individual mice were collected, weighed and gently suspended in PBS containing 0.01% NaN_3. After centrifugation, the supernatants were collected and passed through 0.22-μm filters. The levels of ATP were determined with a luciferin-luciferase assay using an ATP assay kit (TOYO Ink) according to the manufacturer's instructions, except that the cell lysis step was omitted.

Bacterial culture. Faeces were collected from SPF mice, gently dissolved in 10 ml of serum-free RPMI medium, passed through a mesh and incubated under aerobic condition at 37 °C for 16 h. A small aliquot of the faecal suspension was transferred into 3 ml fresh medium and further incubated under aerobic conditions at 37 °C. The growth phases of these culturable intestinal aerobic commensal bacteria were monitored spectrophotometrically at 590 nm, and ATP concentrations in supernatants were measured as above. *S. typhimurium* (obtained from the Research Institute for Microbial Diseases bacterial culture collection, Osaka, Japan) was grown in the same medium, and ATP concentration was measured in the same way. The culture supernatants collected at the late exponential phase of bacterial growth were passed through 0.22-μm filters and used as conditioned media for co-culture of $CD11c^+$ cells and naive $CD4^+$ T cells.

Isolation of lymphocytes. To prepare single-cell suspensions from spleens, mesenteric lymph nodes and Peyer's patches, the collected organs were ground between glass slides, and the cells were passed through 40-μm nylon meshes and suspended in HBSS. Splenocytes were treated with RBC lysis buffer (0.15 M NH_4Cl, 1 mM $KHCO_3$, 0.1 mM EDTA) for 5 min before suspension. Naive $CD4^+$ T cells were purified from spleens using a $CD4^+CD62L^+$ T cell isolation kit II (Miltenyi Biotec; purity 95%). For isolation of lamina propria lymphocytes (see also ref. 3), intestines were opened longitudinally, washed to remove faecal content, and shaken in HBSS containing 5 mM EDTA for 20 min at 37 °C. After removal of epithelial cells and fat tissue, the intestines were cut into small pieces and incubated with RPMI1640 containing 4% fetal bovine serum (FBS), 1 mg ml^{-1} collagenase type II (Invitrogen), 1 mg ml^{-1} dispase (Invitrogen) and 40 μg ml^{-1} DNase I (Roche Diagnostics) for 1 h at 37 °C in a shaking water bath. The digested tissues were washed with HBSS containing 5 mM EDTA, resuspended in 5 ml of 40% Percoll (GE Healthcare) and overlaid on 2.5 ml of 80% Percoll in a 15-ml Falcon tube. Percoll gradient separation was performed by centrifugation at 780*g* for 20 min at 25 °C. The lamina propria lymphocytes were collected at the interface of the Percoll gradient and washed with MACS buffer (0.5% BSA and 2 mM EDTA in PBS) or RPMI1640. The cells were used immediately for experiments.

Isolation of lamina propria $CD11c^+$ cells. Lamina propria $CD11c^+$ cells were isolated using a protocol modified from an EDTA perfusion method[32]. Mice were anesthetized and their peritoneal and pleural cavities opened. Next, 10 ml of 20 mM EDTA in HBSS was perfused through the left ventricle of the heart. At the end of the perfusion, the entire colon or small intestine excluding the caecum was removed, opened longitudinally and washed to remove faecal content. Colons were then cut into halves and placed in tubes filled with 2 mM EDTA in HBSS. The tubes were shaken at 4,800 oscillations per min for 50 s using a mini beater (Biospec Products). The tissues were washed with PBS and the epithelial cells and muscle layers removed with tweezers. In some experiments, the epithelial cell sheets were collected and kept in ice-cold HBSS until RNA extraction. After removal of epithelial cells and muscle layers, the tissues were then cut into small pieces and incubated with RPMI1640 containing 4% FBS, 1 mg ml^{-1} collagenase type II, 1 mg ml^{-1} dispase and 40 μg ml^{-1} DNase I for 1 h at 37 °C in a shaking water bath. After filtration of the digested tissues through a 40-μm cell strainer, the isolated cells were washed with MACS buffer and $CD11c$-positive cells were purified twice to >95% purity using CD11c MicroBeads (Miltenyi Biotec). In some experiments, enriched $CD11c$-positive cells were further stained with specific antibodies and sorted by FACSVantageSE (BD Biosciences), with a resulting purity of around 95%.

Isolation of splenic $CD11c^+$ cells. Spleens were collected and incubated with RPMI1640 containing 4% FBS, 1 mg ml^{-1} collagenase type II, 1 mg ml^{-1} dispase and 40 μg ml^{-1} DNase I for 1 h at 37 °C in a shaking water bath. After treatment with RBC lysis buffer, the isolated cells were washed with MACS buffer and $CD11c$-positive cells purified twice to >95% purity using CD11c MicroBeads (Miltenyi Biotec).

Intracellular cytokine staining. The intracellular expression of IL-17 and IFN-γ in $CD4^+$ T cells was analysed using a Cytofix/Cytoperm Kit Plus (with Golgistop; BD Biosciences) according to the manufacturer's instructions. In brief, lymphocytes obtained from the intestinal lamina propria, spleens, mesenteric lymph nodes or Peyer's patches were incubated with 50 ng ml^{-1} phorbol myristate acetate (PMA; Sigma), 5 μM calcium ionophore A23187 (Sigma) and Golgistop in complete media at 37 °C for 4 h. Surface staining was performed with a corresponding cocktail of fluorescently labelled antibodies for 20 min at 4 °C; after this, the cells were permeabilized with Cytofix/Cytoperm solution for 20 min at 4 °C and intracellular cytokine staining was performed with fluorescently labelled cytokine antibodies for 20 min.

***In vitro* T-cell differentiation.** Naive $CD4^+$ T cells were collected for 4 days with purified $CD11c^+$ cells and 0.5 μg ml^{-1} anti-CD3 antibody (BD Biosciences) in the presence or absence of ATP. The cultured cells were harvested and rested for 2 h before being restimulated with PMA and calcium ionophore (Sigma) for 3 h.

Flow cytometry. The following antibodies were used: anti-CD4-Cychrom, anti-IFN-γ-FITC, anti-IL-17-PE, anti-CD8-FITC, anti-CD11b-PE, anti-CD11b-FITC, anti-CD11c-PE, anti-CD11c-APC, anti-CD80-FITC, anti-CD103-FITC (all BD Biosciences), anti-CCR6-PE (R&D Systems Inc.), anti-F4/80-Alexa488 (Caltag Laboratories), anti-CD70-biotin (eBioscience), rabbit anti-CX3CR1 antibody (Torrey Pines Biolabs), streptavidin-Alexa488 and goat anti-rabbit IgG-Alexa488 (Molecular Probes). Data were acquired using a FACSCalibur or a FACSCanto (BD Biosciences) and analysed using Flowjo software (Tree Star).

Real-time RT–PCR. Complementary DNAs were synthesized from RNA samples prepared with an RNeasy Mini Kit (Qiagen) using Rever Tra Ace (Toyobo). Complementary DNAs were analysed by rRT–PCR using Power SYBR Green PCR Master Mix (Applied Biosystems) in an ABI 7300 real time PCR system (Applied Biosystems). Serial dilutions of a standard were included for each gene to generate a standard curve and allow calculation of the input amount of cDNA for each gene. Values were then normalized by the amount of GAPDH in each sample. The primer sets were designed with Primer Express Version 3.0 (Applied Biosystems) and initially tested to confirm comparable (>90%) efficiencies. The following primer sets were used: *Il17a*, 5′-GGACTCTCCACCGCAATGA-3′ and 5′-GGCACTGAGCTTCCCAGATC-3′; *Il17f*, 5′-CCCCATGGGATTACAACATCAC-3′ and 5′-CATTGATGCAGCCTGAGTGTCT-3′; *Il21*, 5′- GGCAATGAAAGCCTGTGGAA-3′ and 5′- GGCAATGAAAGCCTGTGGAA-3′; *Rorc*, 5′-GGAGGACAGGGAGCCAAGTT-3′ and 5′-CCGTAGTGGATCCCAGATGACT-3′; *Ifng*, 5′-TCAAGTGGCATAGATGTGGAAGAA-3′ and 5′-TGGCTCTGCAGGATTTTCATG-3′; *Il4*, 5′-GGCATTTTGAACGAGGTCACA-3′ and 5′-GACGTTTGGCACATCCATCTC-3′; *Il6*, 5′-CTGCAAGAGACTTCCATCCAGTT-3′ and 5′-AAGTAGGGAAGGCCGTGGTT-3′; *Itgb8*, 5′-ACAGCATCGCATGGACCAA-3′ and 5′-AAGCAACCCGATCAAGAATGTG-3′; *Itgav*, 5′-CGCCTATCTTCGGGATGAATC-3′ and 5′-CCAACCGATACTCCATGAAAATG-3′; *Gapdh*, 5′-CCTCGTCCCGTAGACAAAATG-3′ and 5′-TCTCCACTTTGCCACTGCAA-3′; *P2rx1*, 5′-ACGAAACAAGAAGGTGGGAGT-3′ and 5′-AGGCCACTTGAGGTCTGGTAT-3′; *P2rx2*, 5′-GAGAGCTCCATCATCACCAAA-3′ and 5′-CAGGGTCTGGGAAGGAGTAAC-3′; *P2rx3*, 5′-CCGAGAACTTCACCATTTTCA-3′ and 5′-TTTATGTCCTTGTCGGTGAGG-3′; *P2rx4*, 5′-TGGCTACAATTTCAGGTTTGC-3′ and 5′-GATCATGGTTGGGATGATGTC-3′; *P2rx5*, 5′-AACCGTCTGGACAACAAACAC-3′ and 5′-TTTCATCAGGTCACGGAACTC-3′; *P2rx7*, 5′-CCAGGAAGCAGGAGAGAACTT-3′ and 5′-ATCCGTGTTCTTGTCATCCAG-3′; *P2ry1*, 5′-GGCAGGCTCAAGAAGAAGAAT-3′ and 5′-TCCCAGTGCCAGAGTAGAAGA-3′; *P2ry2*, 5′-CCGAGAGCTCTTTAGCCATTT-3′ and 5′-GCCATAAGCACGTAACAGACC-3′; *P2ry6*, 5′-CTCACCTGCATTAGCTTCCAG-3′ and 5′-ACACGACTCCACACACTACCC-3′; *P2ry12*, 5′-GTTCCTGGGGTTGATAACCAT-3′ and 5′-GCCCAGATGACAACAGAAAGA-3′; *P2ry13*, 5′-CGTTCAGGAAAACCTTTGTCA-3′ and 5′-

ACACTTCTTCACGGATGATGG-3′. The *Tnf*, *Il22* and *Il23a* primer and probe (FAM MGB Probe) were purchased from Applied Biosystems.

ELISA for faecal IgA. Faeces (50–100 mg) were collected from individual mice, weighed and homogenized in 100 μl of PBS containing 0.01% NaN_3 per 10 mg of faeces. After centrifugation at 9,000*g* for 5 min, the supernatants were collected and diluted by 1:1,000. IgA levels were determined by ELISA using a mouse IgA ELISA quantitation kit (Bethyl Laboratories) and TMB solution (eBioscience). Optical densities were determined at a wavelength of 450 nm with a reference wavelength of 570 nm.

T-cell-mediated colitis model. Naive $CD4^+CD62L^{high}$ splenic T cells from Balb/c mice were purified and intraperitoneally transferred into SCID mice (3×10^5 cells per mouse). The mice were then injected with αβ-ATP in RPMI (1.5 mg per mouse) or medium alone every 3 days for 4 weeks. After 8 weeks, the colons were examined for the numbers of IL-17- and IFN-γ-producing $CD4^+$ cells or analysed histologically after haematoxylin and eosin staining.

31. Yamamoto, M. *et al.* Role of adaptor TRIF in the MyD88-independent Toll-like receptor signaling pathway. *Science* **301**, 640–643 (2003).
32. Mizoguchi, E. *et al.* Colonic epithelial functional phenotype varies with type and phase of experimental colitis. *Gastroenterology* **125**, 148–161 (2003).

Potent Antimycobacterial Activity of Mouse Secretory Leukocyte Protease Inhibitor[1]

Junichi Nishimura,*§ Hiroyuki Saiga,*‡ Shintaro Sato,¶ Megumi Okuyama,‖ Hisako Kayama,*‡ Hirotaka Kuwata,* Sohkichi Matsumoto,‖ Toshirou Nishida,§ Yoshiki Sawa,§ Shizuo Akira,¶ Yasunobu Yoshikai,† Masahiro Yamamoto,‡ and Kiyoshi Takeda[2]*‡

Secretory leukocyte protease inhibitor (SLPI) has multiple functions, including inhibition of protease activity, microbial growth, and inflammatory responses. In this study, we demonstrate that mouse SLPI is critically involved in innate host defense against pulmonary mycobacterial infection. During the early phase of respiratory infection with *Mycobacterium bovis* bacillus Calmette-Guérin, SLPI was produced by bronchial and alveolar epithelial cells, as well as alveolar macrophages, and secreted into the alveolar space. Recombinant mouse SLPI effectively inhibited in vitro growth of bacillus Calmette-Guérin and *Mycobacterium tuberculosis* through disruption of the mycobacterial cell wall structure. Each of the two whey acidic protein domains in SLPI was sufficient for inhibiting mycobacterial growth. Cationic residues within the whey acidic protein domains of SLPI were essential for disruption of mycobacterial cell walls. Mice lacking SLPI were highly susceptible to pulmonary infection with *M. tuberculosis*. Thus, mouse SLPI is an essential component of innate host defense against mycobacteria at the respiratory mucosal surface. *The Journal of Immunology*, 2008, 180: 4032–4039.

Mycobacterium tuberculosis is a top killer among bacterial pathogens and is responsible for 2 million deaths annually. The emergence of AIDS and development of multidrug-resistant *M. tuberculosis* have increased the incidence of tuberculosis, and it has now become a serious problem. Therefore, the host defense mechanisms against *M. tuberculosis* have been intensively investigated and important roles of T cell-mediated adaptive immunity are now well established (1, 2). In addition, functional characterization of TLRs has recently indicated the importance of innate immunity in infection with *M. tuberculosis* (3, 4). Macrophages and dendritic cells are the major effectors of TLR-mediated antimycobacterial immune responses, because they produce a variety of proinflammatory cytokines and have the capacity of phagocytosis. However, during *M. tuberculosis* infection, epithelial cells in the respiratory tract as well as alveolar macrophages are the first targets for invasion by *M. tuberculosis*. Therefore, these epithelial cells are expected to play roles in preventing mycobacterial infection by establishing physical barriers and producing proinflammatory and antimicrobial mediators (5).

Secretory leukocyte protease inhibitor (SLPI)[3] is a 12-kDa secreted protein composed of two cysteine-rich whey acidic protein (WAP) domains (also called WAP four-disulfide core (WFDC) domains) (6–8). It was originally identified in seminal fluid and is produced by secretory cells in the genital, respiratory, and lacrimal glands as well as dermal keratinocytes (9–13). SLPI is a potent inhibitor of serine proteases, such as neutrophil elastase and cathepsin G, and has therefore been proposed to protect tissues from protease-mediated damage at sites of inflammation (14, 15). Indeed, SLPI was subsequently shown to mediate wound healing (16, 17). Further studies have revealed that SLPI has additional functions. For example, it possesses an antimicrobial activities against Gram-negative and Gram-positive bacteria, fungi, and viruses, including HIV (18–20). In addition to SLPI, several other serine protease inhibitors containing a single WAP domain, such as Eppin, Elafin, SWAM1, and SWAM2, also possess antimicrobial activities against Gram-negative and Gram-positive bacteria (8, 21, 22). Thus, serine protease inhibitors possessing WAP domains exhibit antimicrobial activities. However, the precise mechanisms by which these serine protease inhibitors exert their antimicrobial activities remain elusive. More recently, SLPI was found to mediate anti-inflammatory responses. Briefly, SLPI is induced in monocytes and macrophages in response to inflammatory stimuli mediated by TLRs (23) and subsequently suppresses TLR-dependent production of inflammatory mediators in macrophages by modulating NF-κB activity (23–25). Consistent with these findings, SLPI-deficient mice are highly sensitive to TLR4 ligand (LPS)-induced endotoxin shock with increased production of IL-6 (26). Thus, SLPI has diverse functions and its precise roles need to be investigated more carefully.

*Deparment of Molecular Genetics and †Division of Host Defense, Research Center for Prevention of Infectious Diseases, Medical Institute of Bioregulation, Kyushu University, Fukuoka; ‡Laboratory of Immune Regulation, Department of Microbiology and Immunology, §Department of Surgery, Graduate School of Medicine, and ¶Department of Host Defense, Research Institute for Microbial Diseases, Osaka University; and ‖Department of Host Defense, Osaka City University Graduate School of Medicine, Osaka, Japan

Received for publication April 3, 2007. Accepted for publication January 9, 2008.

The costs of publication of this article were defrayed in part by the payment of page charges. This article must therefore be hereby marked *advertisement* in accordance with 18 U.S.C. Section 1734 solely to indicate this fact.

[1] This work was supported by a Grant-in-Aid from the Ministry of Education, Culture, Sports, Science and Technology and the Ministry of Health, Labor and Welfare, as well as the Tokyo Biochemical Research Foundation, the Cell Science Research Foundation, the Yakult Bio-Science Foundation, the Osaka Foundation for Promotion of Clinical Immunology, the Sumitomo Foundation, and the Sankyo Foundation of Life Science.

[2] Address correspondence and reprint requests to Dr. Kiyoshi Takeda, Laboratory of Immune Regulation, Department of Microbiology and Immunology, Graduate School of Medicine, Osaka University, Suita, Osaka, 565-0871, Japan. E-mail address: ktakeda@ongene.med.osaka-u.ac.jp

[3] Abbreviations used in this paper: SLPI, secretory leukocyte protease inhibitor; WAP, whey acidic protein; WFDC, WAP four-disulfide core; qPCR, quantitative PCR; BALF, bronchoalveolar lavage fluid; BCG, bacillus Calmette-Guérin; FLUOS, 5-(6-)carboxyfluorescein-*N*-hydroxysuccinimide ester; NPN, 1-*N*-phenylnapthylamine; AEC, alveolar epithelial cell.

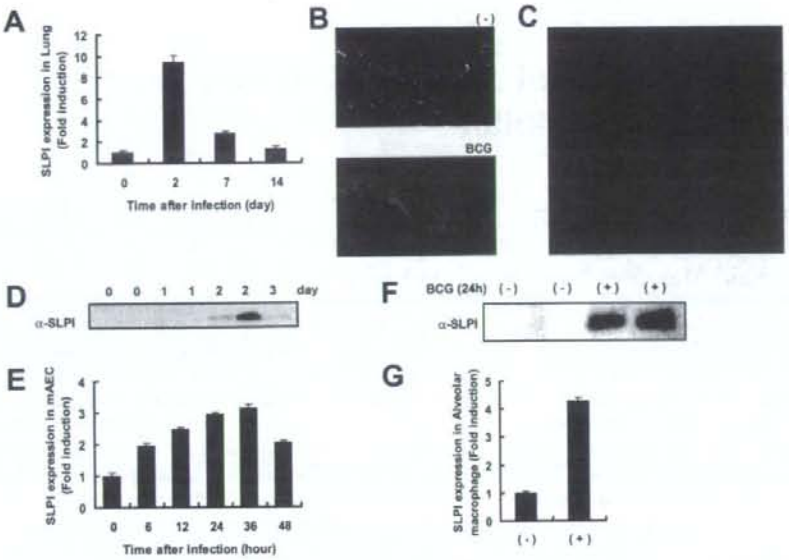

FIGURE 1. Expression of SLPI during mycobacterium infection. *A*, Wild-type mice were intratracheally infected with BCG (4×10^5 CFU). At the indicated periods, total RNA was extracted from the lungs. SLPI mRNA expression was analyzed by quantitative real-time RT-PCR. Data are shown as the relative mRNA levels normalized by the corresponding 18S rRNA level. *B* and *C*, At 2 days after intratracheal infection with BCG, lung tissue sections were stained with an anti-SLPI Ab (red) and 4′,6-diamidino-2-phenylindole (blue) and visualized by fluorescence microscopy. *D*, BALF was collected at the indicated periods after BCG infection. Mouse SLPI protein expression was analyzed by Western blotting with an anti-SLPI Ab. Data obtained from two independent mice (0, 1, and 2 days) are indicated. *E*, AEC were incubated with the same number of BCG for the indicated periods. SLPI mRNA expression was analyzed by quantitative real-time RT-PCR. Data are shown as the relative mRNA levels normalized by the corresponding 18S rRNA level. *F*, AEC were incubated with the same number of BCG. Culture supernatants were collected before (−) and after 24 h of infection (+) and subjected to Western blot analysis using an anti-SLPI Ab. Data obtained from two independent cell clones are shown. *G*, Alveolar macrophages were collected from uninfected wild-type mice, cultured with or without BCG for 48 h, and then analyzed for their SLPI mRNA expression by quantitative real-time RT-PCR. The results are presented as the mean ± SD.

In this study, we investigated the roles of murine SLPI in the context of host defenses against mycobacteria, since SLPI expression is greatly induced in macrophages and the lungs during mycobacterial infection (27). Recombinant SLPI inhibited mycobacterial growth at a lower concentration than that required to inhibit bacterial growth. Inhibition of mycobacterial growth was mediated by increased permeability of the mycobacterial membrane. Mutation of cationic residues in the WAP domains of SLPI resulted in loss of its antimycobacterial activity. Furthermore, SLPI-deficient mice were highly susceptible to pulmonary infection with *M. tuberculosis*. These findings demonstrate that SLPI is a potent antimycobacterial molecule.

Materials and Methods

Cells and bacteria

M. tuberculosis strains H37Ra (ATCC 25177; American Type Culture Collection) and *M. tuberculosis* strains H37Rv (28) were grown in Middlebrook 7H9-ADC medium for 2 wk and stored at −80°C until use. *Mycobacterium bovis* bacillus Calmette-Guérin (BCG; Tokyo strain) was purchased from Kyowa Pharmaceuticals. *Salmonella enterica* serovar *typhimurium* were provided by the Research Institute for Microbial Diseases (Osaka University). For each experiment, the dose was confirmed by plating an aliquot of the injected bacterial suspension. Isolation and immortalization of type II alveolar epithelial cells from the lungs of transgenic H-2K^b-tsA58 mice were performed as previously described (29), with some modifications.

Immunohistochemistry

Lungs were washed with PBS and frozen in Tissue-Tex OCT compound (Sakura, Tokyo, Japan). Cryostat sections (5-μm thick) were fixed with cold acetone for 10 min, dried, rehydrated with PBS, and blocked with PBS containing 20 mM HEPES, 10% FBS, and 1 μg of Fc-blocking mAb (2.4G2; BD Pharmingen). Next, the sections were sequentially incubated with a biotinylated anti-mouse SLPI Ab (R&D Systems) and Alexa Fluor 594-conjugated streptavidin (Molecular Probes). The nuclei were stained with 4′,6-diamidino-2-phenylindole (Molecular Probes). After washing with PBS, the sections were analyzed by confocal microscopy (Zeiss).

Western blot analysis

Samples were boiled for 5 min in reducing SDS-PAGE sample buffer and then subjected to SDS-PAGE. The separated proteins were transferred to a 0.45-μm pore polyvinylidene fluoride membrane (Millipore). After blocking with 5% milk, the membrane was incubated with the above-described biotinylated anti-mouse SLPI Ab (0.2 μg/ml) and a streptavidin-HRP complex (1/10,000 dilution; R&D Systems). The bound Abs were detected by the Super Signal reagent (Pierce).

Quantitative real-time RT-PCR

After isolation of total RNA with the TRIzol reagent (Invitrogen Life Technologies), 4 μg of the RNA was treated with RQ1DNase (Promega) and then reverse-transcribed using Moloney murine leukemia virus reverse transcriptase (Promega) and Random Primers (Toyobo). Gene expression was quantified with an Applied Biosystems PRISM 7000 sequence detection system using TaqMan Universal PCR Master Mix (Applied Biosystems). To determine the relative expression level of each sample, the corresponding 18S rRNA expression level was measured as an internal control. The primer and probe sequences for SLPI were follows: quantitative PCR (qPCR) primer (forward), 5′-d(GCTGTGAGGGTATATGTG GGAAA)-3′; qPCR primer (reverse), 5′-d(CGCCAATGTCAGGGAT CAG)-3′; and qPCR probe, 5′-FAMd(TCTGCCTGCCCCCGATGTG AG)BHQ-3′.

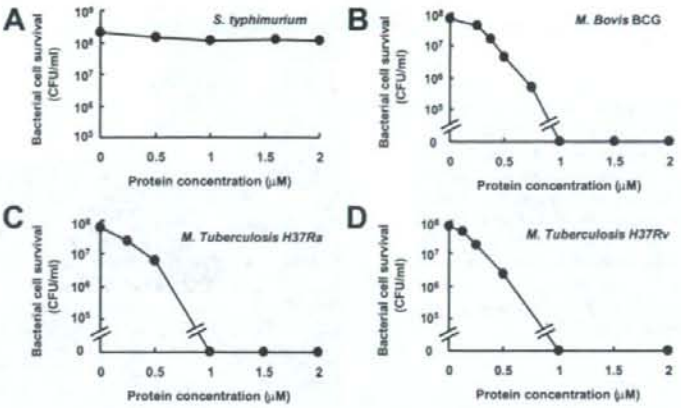

FIGURE 2. Mouse recombinant SLPI inhibits in vitro BCG and *M. tuberculosis* growth. *A*, *S. typhimurium* (5×10^7 CFU/ml) were incubated with SLPI for 2 h and plated on LB agar plates. *B–D*, BCG (*B*), *M. tuberculosis* H37Ra (*C*), or *M. tuberculosis* H37Rv (*D*; 5×10^7 CFU/ml) were incubated with increasing concentrations of recombinant mouse SLPI for 24 h and then plated on 7H10 agar plates.

Bronchoalveolar lavage fluid (BALF)

Mice were intratracheally administered 4×10^5 CFU of BCG suspended in 30 μl of PBS. BALF was collected at the indicated periods. To obtain alveolar macrophages, BALF was centrifuged at 2000 × g for 2 min and the pellet was resuspended in RPMI 1640 containing 4% FBS. The cell count of alveolar macrophages was $\sim 1 \times 10^5$ cells/mouse. To eliminate contamination by bacteria, alveolar macrophages were cultured with 50 U/ml penicillin and 50 μg/ml streptomycin for 16 h, washed five times, and infected with 5×10^7 CFU/well of BCG without penicillin and streptomycin.

Preparation of recombinant SLPI protein and variants

PCR-amplified mouse SLPI cDNA fragments were inserted into pGEX-6P-1 (Amersham Biosciences). pGEX-6P-1 containing mouse SLPI cDNA was transformed into *Escherichia coli* Rosetta-gami B (DE 3). Expression of GST-SLPI fusion proteins was induced by the addition of 1 mM isopropyl-1-thio-β-D-galactoside, and the expressed fusion proteins were purified using glutathione-Sepharose 4B (Amersham Biosciences) according to the manufacturer's instructions. The purified proteins were incubated with PreScission Protease (Amersham Biosciences) at 4°C for 16 h to cleave the GST tag and then purified with glutathione-Sepharose 4B.

Antibacterial activity

Mid-log phase *Salmonella typhimurium* were diluted with PBS containing 1% Luria-Bertani (LB) to give $\sim 5 \times 10^7$ CFU/ml. A final volume of 250 μl was used to examine the antibacterial activities of proteins. After incubation for 2 h, *S. typhimurium* were plated onto LB agar plates. Colonies were counted (CFU/ml) after overnight incubation at 37°C.

Antimycobacterial activity

M. tuberculosis and BCG were grown in Middlebrook 7H9-ADC medium at 37°C with vigorous agitation. After 7 days of incubation, rapidly growing mycobacteria were harvested by centrifugation and adjusted to 5×10^7 CFU/ml in 7H9-ADC medium. After incubation of the mycobacteria with the indicated concentrations of proteins for 24 h at 37°C, serial 20-fold dilutions were conducted in PBS. Aliquots (50 μl) of the dilutions were plated on Middlebrook 7H10 agar plates and incubated at 37°C for 21–28 days. Colonies were counted (CFU/ml) at intervals until no new colonies appeared.

Protein-binding assay

SLPI and BSA were labeled with 5-(and 6-)carboxyfluorescein-*N*-hydroxysuccinimide ester (FLUOS; Roche Diagnostics) as described previously (30). Briefly, 400 μg/ml SLPI or BSA was mixed with 0.096 mg of FLUOS in 1 ml of PBS for 2 h at room temperature. Nonreacted FLUOS was separated by gel filtration using a Sephadex G25 column (Amersham Biosciences). The labeled SLPI or BSA was then incubated with BCG, and the OD at 630 nm was adjusted to 0.2. After 30 min of incubation at 37°C, BCG were washed three times with 7H9 medium containing 0.05% Tween 80. Protein-BCG reactions were detected by confocal laser microscopy (Zeiss).

Scanning electron microscopy

After culture with or without 1 μM SLPI for the indicated times, BCG cultures were fixed with 5% glutaraldehyde, postfixed with 1% osmium tetroxide, dehydrated with ethyl alcohol, treated with isoamyl acetate to replace the alcohol, dried with liquid CO_2 in a critical-point apparatus (HCP-2; Hitachi), and coated with Pt-Pd by ion sputtering (Hitachi) in ion-distilled water. The specimens were analyzed using S-4700 scanning electron microscope (Hitachi), operated at 10 kV.

Outer membrane permeabilization assay

The ability of proteins to permeabilize the outer membranes of BCG was investigated using 1-*N*-phenylnaphthylamine (NPN; Wako Pure Chemical Industries) as described previously (31). Briefly, BCG were suspended in 5 mM HEPES (pH 7.4) containing 10 μM NPN to an OD at 590 nm of 0.15. After incubation at 37°C for 30 min, proteins were added and the fluorescence of NPN was monitored. The excitation wavelength used was 340 nm, and the emission wavelength was 425 nm. The experiment was conducted at 37°C.

Generation of $Slpi^{-/-}$ *mice*

The *Slpi* gene was isolated from genomic DNA extracted from embryonic stem cells (E14.1) by PCR using TaKaRa LA *Taq*. The targeting vector was constructed by replacing a 1.2-kb fragment containing exons 2–4 with a neomycin-resistance gene cassette (*neo*) driven by the PGK promoter and inserting a HSV thymidine kinase into the genomic fragment for negative selection. After transfection of the targeting vector into embryonic stem cells, colonies resistant to both G418 and ganciclovir were selected and screened by PCR and Southern blotting. Homologous recombinants were microinjected into blastocysts of C57BL/6 female mice and heterozygous F_1 progenies were intercrossed to obtain $Slpi^{-/-}$ mice.

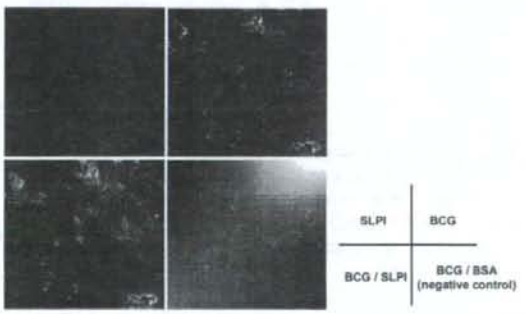

FIGURE 3. SLPI associates with BCG. SLPI and BSA were labeled with FLUOS (Roche). Labeled proteins were incubated with BCG for 30 min, and analyzed by fluorescence microscopy.

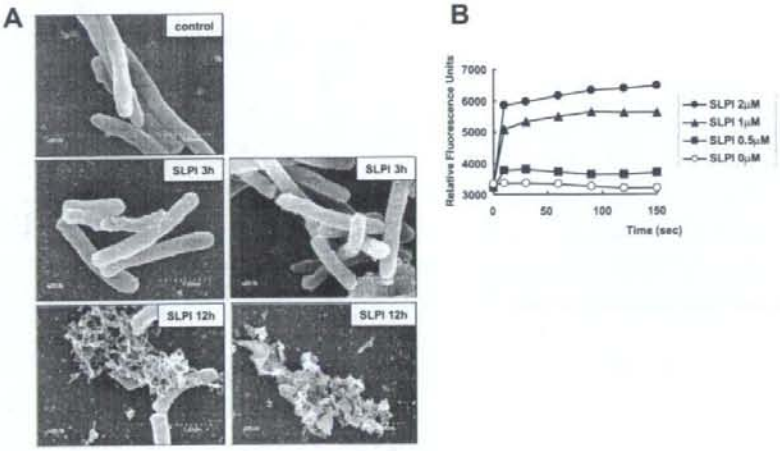

FIGURE 4. SLPI disrupts the BCG cell membrane. *A*, BCG was incubated with or without SLPI for the indicated periods and observed with scanning electron microscopy. *B*, The indicated concentrations of SLPI were added to a BCG suspension containing NPN, and the NPN fluorescence was monitored for the indicated periods. Representative data of three independent experiments are shown.

Slpi$^{-/-}$ mice were backcrossed to C57BL/6 mice for five generations, and *Slpi*$^{-/-}$ and their wild-type littermates from these intercrosses were used for experiments at 6–8 wk of age. All animal experiments were conducted in accordance with the guidelines of the Animal Care and Use Committee of Kyushu University.

In vivo infection

For intratracheal infection, 4×10^5 CFU of *M. tuberculosis* suspended in 30 μl of sterile PBS were administered intratracheally. For i.v. infection, 4×10^5 CFU of *M. tuberculosis* suspended in 100 μl of sterile PBS were administered i.v. At 3 wk after infection, homogenates of the lungs and spleen were plated on 7H10 agar plates. For histological examination, 1×10^7 CFU of *M. tuberculosis* suspended in 30 μl of sterile PBS were administered intratracheally. At 5 days after infection, the lungs were fixed in 4% formalin, embedded in paraffin, cut into sections, and stained with H&E.

Results

SLPI expression in the lungs of BCG-infected mice

To assess the roles of SLPI in mycobacterial infection, we first analyzed SLPI expression in the lungs of mice intratracheally infected with *M. bovis* BCG. Total RNA was extracted from the lungs after 2, 7, and 14 days of infection and analyzed for SLPI mRNA expression by real-time qPCR (Fig. 1*A*). Expression of SLPI mRNA was increased by ~9-fold after 2 days of infection, but decreased thereafter. Next, we analyzed pulmonary cell types expressing SLPI by immunohistochemical analysis (Fig. 1, *B* and *C*). SLPI was detected in bronchial epithelial cells before BCG infection (Fig. 1*B, upper micrograph*). After 2 days of BCG infection, increased amounts of SLPI expression were observed, and mainly localized at the apical side of bronchial epithelial cells (Fig. 1*B, lower micrograph*). This prompted us to investigate whether SLPI was secreted into the alveolar space after BCG infection. Accordingly, BALF was collected from BCG-infected mice and analyzed for SLPI protein expression by Western blotting (Fig. 1*D*). SLPI was not detected in BALF from uninfected mice. After 2 days of BCG infection, SLPI was abundantly detected in BALF from infected mice, indicating that SLPI was secreted into the alveolar space during the early phase of mycobacterial infection. In addition to bronchial epithelial cells, SLPI was expressed in cells of the alveolar area (Fig. 1*C*). Therefore, we isolated type II alveolar epithelial cells (AEC) and alveolar macrophages and analyzed their SLPI expression levels after BCG infection. Since AEC are difficult to culture in vitro, we took advantage of transgenic mice harboring a temperature-sensitive mutation of the SV40 large tumor Ag gene under the control of an IFN-γ-inducible H-2K^b promoter element (32, 33). Using these mice, we successfully established AEC lines expressing surfactant protein C (data not shown).

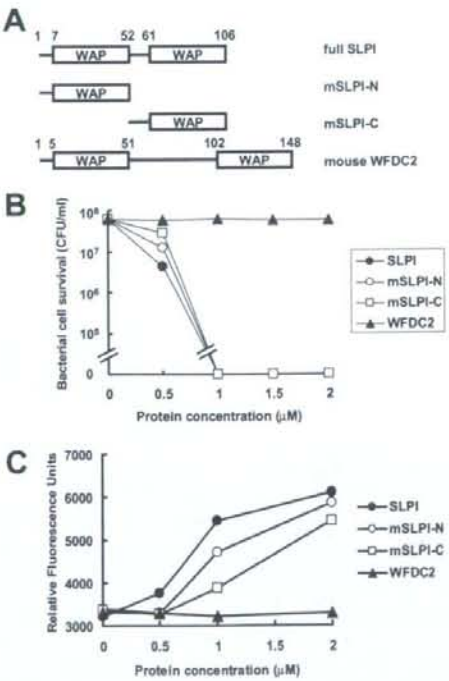

FIGURE 5. A single WAP domain in SLPI is sufficient to inhibit BCG growth. *A*, The deletion mutant constructs mSLPI-N and mSLPI-C lack the C-terminal and N-terminal portions, respectively. White boxes denote WAP domains. *B*, BCG (5×10^7 CFU/ml) was incubated with increasing concentrations of the deletion mutants (mSLPI-N and mSLPI-C) or WFDC2 for 24 h and then plated on 7H10 agar plates. *C*, The indicated concentrations of the deletion mutants (mSLPI-N and mSLPI-C) or WFDC2 were added to BCG suspensions containing NPN. The peak of NPN fluorescence within 150 s was plotted. Representative data of three independent experiments are shown.

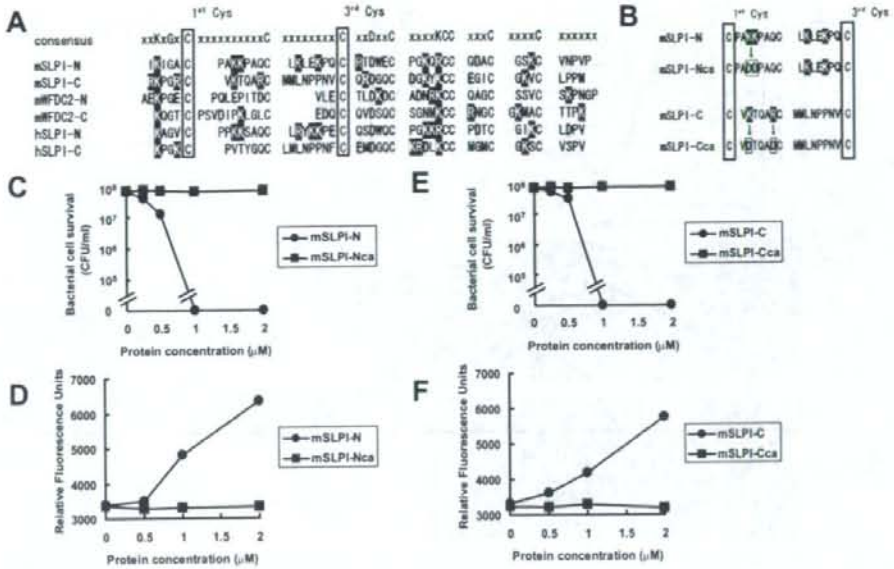

FIGURE 6. Cationic amino acids are responsible for the antimycobacterial activity of SLPI. *A*, Comparison of the WAP domain of SLPI with the WAP domains of other proteins. The consensus amino acid sequence of the WAP domain is shown at the *top* of the protein sequences. Black- and gray-boxed amino acids indicate cationic and anionic amino acids, respectively. Two conserved cysteine residues (first cysteine and third cysteine) are boxed. *B*, Amino acid sequences of the mSLPI-N (mSLPI-Nca) and mSLPI-C (mSLPI-Cca) mutants. *C* and *E*, BCG (5×10^7 CFU/ml) was incubated with increasing concentrations of mSLPI-Nca (*C*) and mSLPI-Cca (*E*) for 24 h and then plated on 7H10 agar plates. *D* and *F*, The indicated concentrations of mSLPI-Nca (*D*) and mSLPI-Cca (*F*) were added to BCG cultures containing NPN. The peak of NPN fluorescence within 150 s was plotted.

AEC were infected with BCG and analyzed for SLPI mRNA expression (Fig. 1*E*). SLPI mRNA expression was gradually induced after BCG infection and peaked after 36 h of infection. AEC have the ability to secrete several effector molecules into the alveolar space. Therefore, we analyzed the SLPI protein levels in culture supernatants from BCG-infected AEC by Western blotting (Fig. 1*F*). SLPI protein was not detected in supernatants from uninfected AEC, but was clearly detected in supernatants after 24 h of BCG infection. Next, isolated alveolar macrophages were infected with BCG and analyzed for SLPI mRNA expression (Fig. 1*G*). BCG infection resulted in an increase in SLPI mRNA expression. Taken together, mycobacterial infection induces the production and secretion of SLPI into the alveolar space by bronchial and type II alveolar epithelial cells as well as alveolar macrophages in the lung.

SLPI-mediated inhibition of mycobacterial growth

Several previous reports have described antimicrobial activities of SLPI against Gram-positive bacteria, Gram-negative bacteria, HIV, and fungi (18–20). However, SLPI needs to be present at high concentrations (>10 μM) for effective inhibition of microbial growth, particularly *S. typhimurium* and *E. coli* (18, 34). Indeed, addition of 2 μM recombinant mouse SLPI only moderately decreased the growth of *S. typhimurium* (Fig. 2*A*). In sharp contrast to the mild inhibition of *S. typhimurium* growth, addition of lower concentrations of mouse SLPI to BCG cultures dramatically reduced the number of CFU (Fig. 2*B*). Growth of BCG was almost completely inhibited by the addition of 1 μM SLPI. A similar inhibitory effect was observed on the growth of *M. tuberculosis* H37Ra and H37Rv (Fig. 2, *C* and *D*). These findings indicate that SLPI has a more potent antimicrobial activity against mycobacteria than against *S. typhimurium*.

Disruption of the BCG cell wall structure by SLPI

Next, we investigated the mechanism of the antimycobacterial activity of SLPI. First, fluorescence-labeled SLPI was incubated with BCG and analyzed by confocal laser microscopy (Fig. 3). BCG and labeled SLPI were colocalized, suggesting that SLPI becomes associated with BCG. We then examined the morphological effects of SLPI on BCG. BCG was incubated with or without SLPI and analyzed by scanning electron microscopy (Fig. 4*A*). BCG exposed to SLPI for 3 h showed pronounced surface blebbing. After 12 h of incubation, many of BCG were collapsed and few live BCG had rough and irregular membrane surfaces. Next, BCG was subjected to an outer membrane permeabilization assay using a fluorescent dye that is weakly fluorescent in aqueous environments but becomes strongly fluorescent in the hydrophobic environment within the cell membrane (Fig. 4*B*). Addition of SLPI caused rapid increases in fluorescence in a dose-dependent manner. These results suggest that SLPI directly associates with mycobacteria, and disrupts the cell wall structure.

Critical role of cationic amino acids in SLPI in its antimycobacterial activity

We next investigated the critical domain involved in the antimycobacterial activity of SLPI. SLPI has two WAP domains (Fig. 5*A*). Several serine protease inhibitors possessing a single WAP domain, such as Eppin, Elafin, SWAM1, and SWAM2, have antimicrobial activities against bacteria such as *E. coli* and *Staphylococcus aureus* (8, 21, 22). To investigate whether each of the WAP domains of mouse SLPI is sufficient to exert antimycobacterial activity, two deletion mutants of SLPI, mSLPI-N and

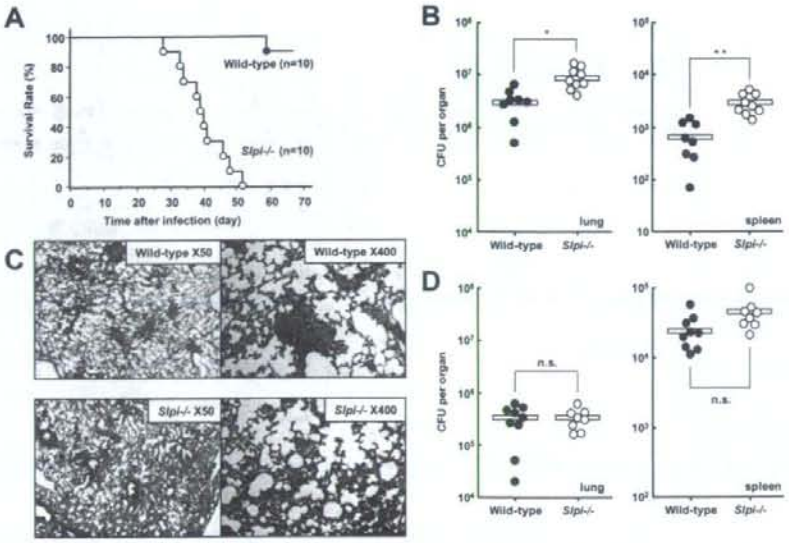

FIGURE 7. *Slpi*$^{-/-}$ mice are highly susceptible to *M. tuberculosis* infection. *A*, *M. tuberculosis* (4×10^5 CFU) were intratracheally infected into wild-type and *Slpi*$^{-/-}$ mice and their survival was monitored. *B*, *M. tuberculosis* (4×10^5 CFU) were intratracheally infected into wild-type and *Slpi*$^{-/-}$ mice. At 3 wk after infection, homogenates of the lungs and spleen were plated on 7H10 agar plates and the CFU titers were counted. Symbols represent individual mice and bars represent the mean of CFU numbers. Statistical analyses were performed using Student's *t* test: *, $p < 0.005$ and **, $p < 0.0005$, significant difference between wild-type and *Slpi*$^{-/-}$ mice. *C*, H&E staining of representative lung tissues from wild-type and *Slpi*$^{-/-}$ mice on day 5 after intratracheal infection with *M. tuberculosis*. *D*, *M. tuberculosis* (4×10^5 CFU) were i.v. infected into wild-type and *Slpi*$^{-/-}$ mice. At 3 wk after infection, homogenates of the lungs and spleen were plated on 7H10 agar plates, and the CFU titers were counted. Symbols represent individual mice and bars represent the mean of CFU numbers. Statistical analyses were performed using Student's *t* test. n.s., Not significant.

mSLPI-C, were generated (Fig. 5*A*). mSLPI-N contained the N-terminal WAP domain, while mSLPI-C contained the C-terminal WAP domain. Both mSLPI-N and mSLPI-C inhibited BCG growth, although their efficiencies were slightly decreased compared with that of full-length SLPI (Fig. 5*B*). Similarly, mSLPI-N and mSLPI-C both induced permeabilization of the outer membrane of BCG with slightly lower efficacies (Fig. 5*C*). These results imply that each WAP domain of mouse SLPI exhibits antimycobacterial activity by disrupting the mycobacterial cell wall structure. WFDC2 is a secreted protein possessing two WAP domains (Fig. 5*A*) (35). However, recombinant mouse WFDC2 had no effect on mycobacterial growth and did not induce permeabilization of the BCG cell membrane, indicating that not all WAP domain-containing proteins have antimicrobial activities (Fig. 5, *B* and *C*). In addition, the N-terminal, but not the C-terminal, WAP domain of human SLPI has been shown to mediate its antimicrobial activities against *E. coli* and *S. aureus* (18). Therefore, we compared the amino acid sequences of the WAP domains of mouse and human SLPI as well as mouse WFDC2 (Fig. 6*A*). The C-terminal regions were conserved among all of the WAP domains. However, the sequences between the first and third cysteine residues were less conserved. In particular, when we examined the sequences between the first and second cysteine residues, we noted that the WAP domains possessing antimycobacterial activities (mSLPI-N, mSLPI-C, and hSLPI-N) contained two or more cationic amino acids, whereas the WAP domains with no antimycobacterial activities (mWFDC2-N, mWFDC2-C, and hSLPI-C) had one or zero cationic acids and instead contained anionic amino acids. Therefore, we produced mSLPI-N (mSLPI-Nca) and mSLPI-C (mSLPI-Cca) mutants, in which the two cationic amino acids were changed to the anionic amino acid aspartic acid (Fig. 6*B*). Neither mSLPI-Nca nor mSLPI-Cca was able to inhibit BCG growth or permeabilize the cell membrane (Fig. 6, *C–F*). These results suggest that the cationic acids of mouse SLPI are responsible for its potent antimycobacterial activities.

High susceptibility of SLPI-deficient mice to M. tuberculosis *infection*

In the next experiment, we assessed the physiological roles of SLPI during mycobacterial infection by generating mice lacking SLPI (*Slpi*$^{-/-}$ mice) via gene targeting (data not shown). First, wild-type and *Slpi*$^{-/-}$ mice were intratracheally infected with *M. tuberculosis* H37Ra, and monitored for their survival (Fig. 7*A*). All *Slpi*$^{-/-}$ mice died within 8 wk of infection at a dose that almost all wild-type mice survived for >9 wk. Next, we counted CFU numbers in the lungs and spleen after 3 wk of infection (Fig. 7*B*). The CFU titers of *M. tuberculosis* in both tissues were higher for *Slpi*$^{-/-}$ mice than that for wild-type mice. The histopathological changes in the lungs after 5 days of *M. tuberculosis* infection were also analyzed (Fig. 7*C*). In wild-type mice, the formation of several small granulomas was observed. In contrast, granulomatous changes were induced to a lesser extent in *Slpi*$^{-/-}$ mice and rather diffuse cell infiltration was observed instead. Next, mice were i.v. infected with *M. tuberculosis*, and the CFU numbers in the lungs and spleen were counted after 3 wk of infection (Fig. 7*D*). The CFU titers were not as dramatically increased in both tissues of *Slpi*$^{-/-}$ mice compared with the corresponding titers in the tissues of wild-type mice, indicating that *Slpi*$^{-/-}$ mice are not highly susceptible to i.v. *M. tuberculosis* infection. Taken together, these findings indicate that *Slpi*$^{-/-}$ mice are highly vulnerable to *M. tuberculosis* infection via the respiratory route.

Discussion

In the present study, we analyzed the roles of mouse SLPI in host defense against mycobacteria. During the early phase of respiratory mycobacterial infection, SLPI was produced and secreted into the alveolar space by bronchial and type II alveolar epithelial cells as well as alveolar macrophages. Recombinant mouse SLPI inhibited the growth of mycobacteria more effectively than it inhibited the growth of Gram-negative bacteria. The SLPI-mediated inhibition of mycobacterial growth was attributable to disruption of the mycobacterial cell wall structure. Furthermore, *Slpi*$^{-/-}$ mice were highly susceptible to pulmonary *M. tuberculosis* infection, highlighting a mandatory role for mouse SLPI in the host defense against *M. tuberculosis* infection. Thus, mouse SLPI is a critical antimycobacterial molecule that acts during the early phase of mycobacterial infection at the respiratory mucosal surface.

Similar structural changes to those observed in SLPI-treated mycobacterial cell walls were induced in several bacteria and *M. tuberculosis* treated with the antimicrobial peptides defensins, which permeabilize microbial membranes (36, 37). We further identified the critical elements for the potent antimycobacterial activity of mouse SLPI. It has been proposed that defensins containing positively charged amino acid residues associate with microorganisms by targeting the surface-exposed negatively charged phospholipid head groups in the microbial membrane (37). Indeed, mutations that change arginine to aspartic acid can attenuate the bactericidal activity of the α-defensin cryptdin-4 (38). Therefore, we supposed that SLPI, which has similar effects on mycobacterial membranes to defensins, also associates with negatively charged mycobacterial membranes through its positively charged amino acid residues. Consistent with this hypothesis, the sequences between the first and second conserved cysteine residues of the WAP domains are not conserved. Moreover, there are several positively charged amino acids (lysine and arginine) in these regions of the WAP domains that possess antimicrobial activities, whereas the regions without any antimicrobial activities contain one or zero positively charged amino acids. Furthermore, structural studies have revealed that the region between the first and second conserved cysteine residues is exposed on the outside of the molecule, thereby enabling this region to associate with microbial membranes (39, 40). Indeed, mutations of the cationic amino acid residues within this region resulted in elimination of the antimycobacterial activity. Thus, mouse SLPI exhibits antimycobacterial activity in quite a similar manner to that of defensins.

In comparison to SLPI, higher concentrations of other serine protease inhibitors containing a WAP domain are required to inhibit microbial growth (8, 21, 22). Recombinant human SLPI is less effective at inhibiting the growth of mycobacteria and *S. typhimurium* (our unpublished data). These differential properties may be attributable to structural differences in the WAP domains, which mediate the antimicrobial activity. SLPI has two WAP domains, whereas other serine protease inhibitors, such as Eppin, Elafin, and SWAMs, have only a single WAP domain. In the case of human SLPI, only the N-terminal WAP domain exhibits antimicrobial activity (18). In addition, only the N-terminal WAP domain of human SLPI contains critical cationic acid residues. The presence of two WAP domains possessing antimicrobial activity may be responsible for the high potency of mouse SLPI for mycobacterial growth inhibition.

Mouse SLPI inhibited mycobacterial growth at profoundly lower concentrations than those required to inhibit the growth of *S. typhimurium* or other microorganisms (18–20). It remains unclear how SLPI becomes more specifically targeted toward mycobacteria. Differential antimicrobial properties against distinct microorganisms have not been reported in the case of defensins. Therefore, SLPI, which has multifunctional properties, may have an unknown strategy for specifically recognizing mycobacteria.

The in vitro findings demonstrating that mouse SLPI inhibits mycobacterial growth were further strengthened by in vivo studies using *Slpi*$^{-/-}$ mice. *Slpi*$^{-/-}$ mice were highly susceptible to pulmonary *M. tuberculosis* infection, but not to i.v. infection. In accordance with this finding, SLPI protein was abundantly detected in the alveolar space after pulmonary BCG infection, but was not detected in sera from mice after i.v. BCG infection (our unpublished data). Therefore, high concentrations of SLPI are supposed to be secreted into the alveolar space during the early phase of respiratory infection with *M. tuberculosis*, thereby promptly killing the mycobacteria before they can invade the lung tissues through the epithelial barrier. Given that mouse SLPI has potent antimycobacterial activities, it would be a good candidate for treatment during the acute phase of *M. tuberculosis* infection and may even be able to be used for the treatment of patients with multidrug-resistant *M. tuberculosis*.

Acknowledgments

We thank S. Ehrt and A. Ding for helpful discussions, Y. Yamada and K. Takeda for technical assistance, and M. Kurata for secretarial assistance.

Disclosures

The authors have no financial conflict of interest.

References

1. Kaufmann, S. H. 2006. Tuberculosis: back on the immunologists' agenda. *Immunity* 24: 351–357.
2. North, R. J., and Y. J. Jung. 2004. Immunity to tuberculosis. *Annu. Rev. Immunol.* 22: 599–623.
3. Fremond, C. M., V. Yeremeev, D. M. Nicolle, M. Jacobs, V. F. Quesniaux, and B. Ryffel. 2004. Fatal *Mycobacterium tuberculosis* infection despite adaptive immune response in the absence of MyD88. *J. Clin. Invest.* 114: 1790–1799.
4. Quesniaux, V., C. Fremond, M. Jacobs, S. Parida, D. Nicolle, V. Yeremeev, F. Bihl, F. Erard, T. Botha, M. Drennan, et al. 2004. Toll-like receptor pathways in the immune responses to mycobacteria. *Microbes Infect.* 6: 946–959.
5. Gerritsen, J. 2000. Host defence mechanisms of the respiratory system. *Paediatr. Respir. Rev.* 1: 128–134.
6. Clauss, A., H. Lilja, and A. Lundwall. 2005. The evolution of a genetic locus encoding small serine proteinase inhibitors. *Biochem. Biophys. Res. Commun.* 333: 383–389.
7. Eisenberg, S. P., K. K. Hale, P. Heimdal, and R. C. Thompson. 1990. Location of the protease-inhibitory region of secretory leukocyte protease inhibitor. *J. Biol. Chem.* 265: 7976–7981.
8. Hagiwara, K., T. Kikuchi, Y. Endo, Huqun, K. Usui, M. Takahashi, N. Shibata, T. Kusakabe, H. Xin, S. Hoshi, et al. 2003. Mouse SWAM1 and SWAM2 are antibacterial proteins composed of a single whey acidic protein motif. *J. Immunol.* 170: 1973–1979.
9. Abe, T., N. Kobayashi, K. Yoshimura, B. C. Trapnell, H. Kim, R. C. Hubbard, M. T. Brewer, R. C. Thompson, and R. G. Crystal. 1991. Expression of the secretory leukoprotease inhibitor gene in epithelial cells. *J. Clin. Invest.* 87: 2207–2215.
10. Hiemstra, P. S., S. van Wetering, and J. Stolk. 1998. Neutrophil serine proteinases and defensins in chronic obstructive pulmonary disease: effects on pulmonary epithelium. *Eur. Respir. J.* 12: 1200–1208.
11. Schiessler, H., E. Fink, and H. Fritz. 1976. Acid-stable proteinase inhibitors from human seminal plasma. *Methods Enzymol.* 45: 847–859.
12. Vogelmeier, C., R. C. Hubbard, G. A. Fells, H. P. Schnebli, R. C. Thompson, H. Fritz, and R. G. Crystal. 1991. Anti-neutrophil elastase defense of the normal human respiratory epithelial surface provided by the secretory leukoprotease inhibitor. *J. Clin. Invest.* 87: 482–488.
13. Wingens, M., B. H. van Bergen, P. S. Hiemstra, J. F. Meis, I. M. van Vlijmen-Willems, P. L. Zeeuwen, J. Mulder, H. A. Kramps, F. van Ruissen, and J. Schalkwijk. 1998. Induction of SLPI (ALP/HUSI-I) in epidermal keratinocytes. *J. Invest. Dermatol.* 111: 996–1002.
14. Gauthier, F., U. Fryksmark, K. Ohlsson, and J. G. Bieth. 1982. Kinetics of the inhibition of leukocyte elastase by the bronchial inhibitor. *Biochim. Biophys. Acta* 700: 178–183.
15. Thompson, R. C., and K. Ohlsson. 1986. Isolation, properties, and complete amino acid sequence of human secretory leukocyte protease inhibitor, a potent inhibitor of leukocyte elastase. *Proc. Natl. Acad. Sci. USA* 83: 6692–6696.
16. Ashcroft, G. S., K. Lei, W. Jin, G. Longenecker, A. B. Kulkarni, T. Greenwell-Wild, H. Hale-Donze, G. McGrady, X. Y. Song, and S. M. Wahl. 2000. Secretory leukocyte protease inhibitor mediates non-redundant functions necessary for normal wound healing. *Nat. Med.* 6: 1147–1153.

17. Zhu, J., C. Nathan, W. Jin, D. Sim, G. S. Ashcroft, S. M. Wahl, L. Lacomis, H. Erdjument-Bromage, P. Tempst, C. D. Wright, and A. Ding. 2002. Conversion of proepithelin to epithelins: roles of SLPI and elastase in host defense and wound repair. *Cell* 111: 867–878.
18. Hiemstra, P. S., R. J. Maassen, J. Stolk, R. Heinzel-Wieland, G. J. Steffens, and J. H. Dijkman. 1996. Antibacterial activity of antileukoprotease. *Infect. Immun.* 64: 4520–4524.
19. McNeely, T. B., D. C. Shugars, M. Rosendahl, C. Tucker, S. P. Eisenberg, and S. M. Wahl. 1997. Inhibition of human immunodeficiency virus type 1 infectivity by secretory leukocyte protease inhibitor occurs prior to viral reverse transcription. *Blood* 90: 1141–1149.
20. Tomee, J. F., P. S. Hiemstra, R. Heinzel-Wieland, and H. F. Kauffman. 1997. Antileukoprotease: an endogenous protein in the innate mucosal defense against fungi. *J. Infect. Dis.* 176: 740–747.
21. Simpson, A. J., A. I. Maxwell, J. R. Govan, C. Haslett, and J. M. Sallenave. 1999. Elafin (elastase-specific inhibitor) has anti-microbial activity against Gram-positive and Gram-negative respiratory pathogens. *FEBS Lett.* 452: 309–313.
22. Yenugu, S., R. T. Richardson, P. Sivashanmugam, Z. Wang, M. G. O'Rand, F. S. French, and S. H. Hall. 2004. Antimicrobial activity of human EPPIN, an androgen-regulated, sperm-bound protein with a whey acidic protein motif. *Biol. Reprod.* 71: 1484–1490.
23. Jin, F. Y., C. Nathan, D. Radzioch, and A. Ding. 1997. Secretory leukocyte protease inhibitor: a macrophage product induced by and antagonistic to bacterial lipopolysaccharide. *Cell* 88: 417–426.
24. Taggart, C. C., S. A. Cryan, S. Weldon, A. Gibbons, C. M. Greene, E. Kelly, T. B. Low, S. J. O'Neill, and N. G. McElvaney. 2005. Secretory leucoprotease inhibitor binds to NF-κB binding sites in monocytes and inhibits p65 binding. *J. Exp. Med.* 202: 1659–1668.
25. Taggart, C. C., C. M. Greene, N. G. McElvaney, and S. O'Neill. 2002. Secretory leucoprotease inhibitor prevents lipopolysaccharide-induced IκBα degradation without affecting phosphorylation or ubiquitination. *J. Biol. Chem.* 277: 33648–33653.
26. Nakamura, A., Y. Mori, K. Hagiwara, T. Suzuki, T. Sakakibara, T. Kikuchi, T. Igarashi, M. Ebina, T. Abe, J. Miyazaki, et al. 2003. Increased susceptibility to LPS-induced endotoxin shock in secretory leukoprotease inhibitor (SLPI)-deficient mice. *J. Exp. Med.* 197: 669–674.
27. Ding, A., H. Yu, J. Yang, S. Shi, and S. Ehrt. 2005. Induction of macrophage-derived SLPI by *Mycobacterium tuberculosis* depends on TLR2 but not MyD88. *Immunology* 116: 381–389.
28. Doi, T., H. Yamada, T. Yajima, W. Wajjwalku, T. Hara, and Y. Yoshikai. 2007. H2-M3-restricted CD8$^+$ T cells induced by peptide-pulsed dendritic cells confer protection against *Mycobacterium tuberculosis*. *J. Immunol.* 178: 3806–3813.
29. deMello, D. E., S. Mahmoud, P. J. Padfield, and J. W. Hoffmann. 2000. Generation of an immortal differentiated lung type-II epithelial cell line from the adult H-2K^{b}tsA58 transgenic mouse. *In Vitro Cell. Dev. Biol. Anim.* 36: 374–382.
30. Aoki, K., S. Matsumoto, Y. Hirayama, T. Wada, Y. Ozeki, M. Niki, P. Domenech, K. Umemori, S. Yamamoto, A. Mineda, et al. 2004. Extracellular mycobacterial DNA-binding protein 1 participates in mycobacterium-lung epithelial cell interaction through hyaluronic acid. *J. Biol. Chem.* 279: 39798–39806.
31. Loh, B., C. Grant, and R. E. Hancock. 1984. Use of the fluorescent probe 1-*N*-phenylnaphthylamine to study the interactions of aminoglycoside antibiotics with the outer membrane of *Pseudomonas aeruginosa*. *Antimicrob. Agents Chemother.* 26: 546–551.
32. Jat, P. S., M. D. Noble, P. Ataliotis, Y. Tanaka, N. Yannoutsos, L. Larsen, and D. Kioussis. 1991. Direct derivation of conditionally immortal cell lines from an H-2K^b-tsA58 transgenic mouse. *Proc. Natl. Acad. Sci. USA* 88: 5096–5100.
33. Whitehead, R. H., P. E. VanEeden, M. D. Noble, P. Ataliotis, and P. S. Jat. 1993. Establishment of conditionally immortalized epithelial cell lines from both colon and small intestine of adult H-2K^b-tsA58 transgenic mice. *Proc. Natl. Acad. Sci. USA* 90: 587–591.
34. Si-Tahar, M., D. Merlin, S. Sitaraman, and J. L. Madara. 2000. Constitutive and regulated secretion of secretory leukocyte proteinase inhibitor by human intestinal epithelial cells. *Gastroenterology* 118: 1061–1071.
35. Kirchhoff, C., I. Habben, R. Ivell, and N. Krull. 1991. A major human epididymis-specific cDNA encodes a protein with sequence homology to extracellular proteinase inhibitors. *Biol. Reprod.* 45: 350–357.
36. Miyakawa, Y., P. Ratnakar, A. G. Rao, M. L. Costello, O. Mathieu-Costello, R. I. Lehrer, and A. Catanzaro. 1996. In vitro activity of the antimicrobial peptides human and rabbit defensins and porcine leukocyte protegrin against *Mycobacterium tuberculosis*. *Infect. Immun.* 64: 926–932.
37. Zasloff, M. 2002. Antimicrobial peptides of multicellular organisms. *Nature* 415: 389–395.
38. Tanabe, H., X. Qu, C. S. Weeks, J. E. Cummings, S. Kolusheva, K. B. Walsh, R. Jelinek, T. K. Vanderlick, M. E. Selsted, and A. J. Ouellette. 2004. Structure-activity determinants in Paneth cell α-defensins: loss-of-function in mouse cryptdin-4 by charge-reversal at arginine residue positions. *J. Biol. Chem.* 279: 11976–11983.
39. Grutter, M. G., G. Fendrich, R. Huber, and W. Bode. 1988. The 2.5 A X-ray crystal structure of the acid-stable proteinase inhibitor from human mucous secretions analysed in its complex with bovine α-chymotrypsin. *EMBO J.* 7: 345–351.
40. Lin, C. C., and J. Y. Chang. 2006. Pathway of oxidative folding of secretory leucocyte protease inhibitor: an 8-disulfide protein exhibits a unique mechanism of folding. *Biochemistry* 45: 6231–6240.